



Article

Design and Evaluation of a Smart Ex Vitro Acclimatization System for Tissue Culture Plantlets

Maged Mohammed^{1,2,*} , Muhammad Munir¹ and Hesham S. Ghazzawy^{1,3} ¹ Date Palm Research Center of Excellence, King Faisal University, Al-Ahsa 31982, Saudi Arabia² Department of Agricultural and Biosystems Engineering, Faculty of Agriculture, Menoufia University, Shebin El Koum 32514, Egypt³ Central Laboratory for Date Palm Research and Development, Agriculture Research Center, Giza 12511, Egypt

* Correspondence: memohammed@kfu.edu.sa

Abstract: One of the technological advancements in agricultural production is the tissue culture propagation technique, commonly used for mass multiplication and disease-free plants. The necessity for date palm tissue culture emerged from the inability of traditional propagation methods' offshoots to meet the immediate demands for significant amounts of planting material for commercial cultivars. Tissue culture plantlets are produced in a protected aseptic in vitro environment where all growth variables are strictly controlled. The challenges occur when these plantlets are transferred to an ex vitro climate for acclimatization. Traditional glasshouses are frequently used; however, this has substantial mortality consequences. In the present study, a novel IoT-based automated ex vitro acclimatization system (E-VAS) was designed and evaluated for the acclimatization of date palm plantlets (cv. Khalas) to enhance their morpho-physiological attributes and reduce the mortality rate and the contamination risk through minimal human contact. The experimental findings showed that the morpho-physiological parameters of 6- and 12-month-old plants were higher when acclimatized in the prototype E-VAS compared to the traditional glasshouse acclimatization system (TGAS). The maximum plant mortality percentage occurred within the first month of the transfer from the in vitro to ex vitro environment in both systems, which gradually declined up to six months; after that, no significant plant mortality was observed. About 6% mortality was recorded in E-VAS, whereas 18% in TGAS within the first month of acclimatization. After six months of study, an overall 14% mortality was recorded in E-VAS compared to 41% in TGAS. The proposed automated system has a significant potential to address the growing demand for the rapid multiplication of tissue culture-produced planting materials since the plant survival rate and phenotype quality were much higher in E-VAS than in the conventional manual system that the present industry follows for commercial production.

Keywords: climate automation; cloud-based IoT; date palm; greenhouse; in vitro; real-time monitoring; sensors; smart agriculture; ThingSpeak



Citation: Mohammed, M.; Munir, M.; Ghazzawy, H.S. Design and Evaluation of a Smart Ex Vitro Acclimatization System for Tissue Culture Plantlets. *Agronomy* **2023**, *13*, 78. <https://doi.org/10.3390/agronomy13010078>

Academic Editors: Jorge García Morillo, Emilio Camacho Poyato and Juan Manuel Díaz-Cabrera

Received: 3 November 2022

Revised: 21 December 2022

Accepted: 23 December 2022

Published: 26 December 2022



Copyright: © 2022 by the authors. Licensee MDPI, Basel, Switzerland. This article is an open access article distributed under the terms and conditions of the Creative Commons Attribution (CC BY) license (<https://creativecommons.org/licenses/by/4.0/>).

1. Introduction

Dioecious date palm (*Phoenix dactylifera* L.) sexual propagation results in high genetic heterozygous progeny, making it unsuitable for commercial utilization [1]. The commercial date palm cultivars are therefore reproduced by asexual propagation methods. Despite its restricted availability and slow development, offshoots give consideration to its conventional vegetative propagation. The offshoots are also doomed to failure if separated from the mother palm due to insufficient root growth [2,3]. The tissue culture propagation method, also known as the in vitro technique, has emerged as a successful substitute for traditional methods of propagation and is widely used to produce large numbers of genetically identical, physiologically superior, and phytosanitary plants in a limited time and space from a single mother plant [4]. It is carried out in a controlled, regulated environment, which also completely removes the chance of any disruption to the growing season [5]. In vitro propagation techniques can be used to produce a variety of herbaceous monocotyledon plants.

However, *in vitro* vegetative woody monocotyledon propagation reports are few [6–8]. The *in vitro* propagation approach is preferred to produce disease-free monocotyledonous date palms in large numbers of true-to-type in a short period [9–12]. In this propagation method, explants of the date palm shoot tip, lateral buds, or inflorescences are used successfully for regeneration [13–16]. Direct organogenesis or somatic embryo-genesis techniques are used to regenerate the *in vitro* date palm plantlets using these explants [17–19].

Many *in vitro*-derived plants still face a considerable barrier during the transplantation phase. Plantlets that have been cultivated *in vitro* have been continuously exposed to a unique, stress-free aseptic microenvironment. Plantlets were grown in test tubes or flasks under controlled conditions, such as high humidity, low light, asepsis, and sugar- and nutrient-rich environments that encouraged heterotrophic development [20,21]. If these plantlets are continuously developed in such a setting, they develop abnormal morphology, anatomy, and physiology. These plantlets develop a culture-induced phenotype that cannot withstand the ambient environmental conditions when planted directly in a glasshouse. In this environment, the plantlets switch from a heterotrophic to an autotrophic metabolism, making them particularly vulnerable to external diseases and climate factors [22,23]. The production of many economically useful crop species is significantly hampered by *in vitro* recalcitrance [24,25]; however, substantial research has been conducted to improve the *in vitro* environment. There is, however, little information on how to acclimate plants grown *in vitro* to the *ex vitro* soil environment [26]. Acclimatization is the process by which a plant adapts to the climatic or environmental conditions of a new habitat [27]. It is the crucial last stage in the tissue culture technique, and the key to successful plant propagation [26]. Plantlets must rectify their morphological, anatomical, and physiological abnormalities after being transferred from an *in vitro* to an *ex vitro* environment before moving to an *in vivo* condition. In the glasshouse, the plantlet quickly wilts because of the much higher irradiance, significantly lower air humidity, and higher substrate water potential, all of which contribute to the leaves' unrestricted water loss. The absence of well-developed epicuticular waxes is common in leaves that grow *in vitro*, which prevents stomata from closing normally and may reduce photosynthetic efficiency [28–31]. Plantlets can be hardened in the test tubes or after transplantation to accelerate acclimatization [32] by lowering transpiration rates with antitranspirants such as abscisic acid or increasing the photosynthetic rate by raising CO₂ concentration [33,34]. Due to its poor ability to prevent water loss through leaf transpiration in the *ex vitro* environment, the plant may incur substantial stress [20,35]. Building a healthy root system is crucial for *in vitro*-grown plantlets to survive after transplantation. The newly *in vitro*-developed roots cannot absorb water and solutes and cannot immediately counteract the rate at which leaves are transpiring [36,37]. Additionally, photosynthesis is still constrained since it depends mainly on the reserves accumulated in *in vitro* media. Therefore, when plantlets are transferred to the *ex vitro* environment, carbon balance may also become a limiting factor and negatively impact photosynthesis [38,39].

Traditionally, when the *in vitro* organogenesis procedure is completed and the date palm plantlets are around 8 to 10 cm in size, they are moved to a glasshouse for acclimatization. After that, they are planted into pots filled with a mixture of sand, peat moss, perlite, and vermiculite. To facilitate the transition from an *in vitro* environment to an ambient one, the potted plants are kept for a few weeks inside a glasshouse in an enclosed plastic tunnel [40]. The plantlets are further hardened after their initial adaptation in the plastic tunnel until they reach 25–30 cm in height and have 3–5 leaves in the glasshouse environment [17,19,41]. A significant percentage of *in vitro*-derived plantlets do not survive when moved from a controlled *in vitro* environment to an ambient glasshouse or outdoor conditions [39,42], because the juvenile *in vitro* plantlets are under stress since the glasshouse environment has much lower relative humidity (RH), high irradiation, and aseptic conditions [22,43,44].

Innovative technologies are becoming increasingly indispensable in the agriculture sector as a tool for sustainable development [45]. Agriculture automation has lowered pro-

duction costs, reduced manual labor, improved environmental sustainability, and enhanced product quality. The productivity of agriculture was significantly boosted by automated farming equipment, glasshouse climate control, irrigation and fertigation systems, soil fertility, and pest and disease control [46–50]. Automation is a practical strategy since *in vitro* propagation necessitates a lot of repetitive effort and is time-consuming, especially if the output is kept to a minimum during the acclimation period due to plantlet mortality. Reduced contamination risk and decreased labor cost are two additional advantages of automating the acclimatization process [51–54]. Modern precision agriculture practices, including glasshouse technology, are largely automated, and information technology paired with IoT (internet of things) technology is well-developed and efficient. Although the idea of the IoT is not new, it has only recently been put into practice, largely due to advancements in hardware technology over the past decade. Robots, drones, remote sensors, computer imagery, and continuously improving machine learning and analytical tools are used in the IoT to real-time monitor crops, microclimate, survey and map fields as well as to provide data to farmers for logical farm management strategies that will not only save them time and money but also improve crop production [55–57]. While maintaining the economic stability of farming enterprises, IoT technology is increasingly being used in agriculture to promote greener on-farm practices and better ecological sustainability [58–60]. Many automated IoT-based technologies that are widely used in plant tissue culture laboratories have been developed by scientists. In a laboratory for banana tissue culture, an automated IoT system was successfully tested to regulate temperature and RH [61]. A prototype automated IoT system was designed and installed in a tissue culture laboratory of sugarcane to monitor and regulate temperature, RH, and light intensity. In the same system, an artificial intelligence-based plant health prediction system also detected the contamination of sugarcane crops [62]. An automated IoT system was successfully developed to monitor the environment of a tissue culture laboratory for mushrooms in order to reduce culture failure [63].

Research studies have used technological innovations to automate and regulate tissue culture laboratories. However, limited research has been conducted on the IoT-based monitoring and control of *ex vitro* conditions during acclimatization. The newly established test tube plantlets are more vulnerable to the ambient environment. Plantlets can rapidly desiccate, wilt, or even die due to environmental change if considerable precautions are not made to accommodate them when transitioning from *in vitro* to *ex vitro* conditions. This commercial *in vitro* propagation stage is often the limiting factor because of the labor and cost associated with traditional glasshouse acclimatization. In order to increase the plant survival rate and to enhance the morpho-physiological traits of newly established *in vitro* date palm plantlets, we designed and evaluated a smart IoT-based *ex vitro* acclimatization system and compared it to the traditional glasshouse acclimatization system. The aim of the proposed smart IoT-based *ex vitro* acclimatization system was to minimize the initial shock of newly regenerated *in vitro* plantlets, which will decrease their mortality and improve their growth characteristics. Moreover, the proposed IoT-based automated system can be used commercially in the glasshouse to reduce plantlet mortality and promote plant characteristics.

2. Materials and Methods

2.1. Description of the Ex Vitro Acclimatization System

The smart *ex vitro* acclimatization system (E-VAS) was designed and implemented at Date Palm Research Center of Excellence (DPRC), King Faisal University (KFU), Saudi Arabia (Latitude: 25.3357° N, Longitude: 49.5952° E). The E-VAS performance was evaluated and compared to the traditional glasshouse acclimatization system (TGAS). The E-VAS consisted of seven main units, i.e., the thermally insulated acclimatization chamber, the heating unit, the cooling unit, the humidification unit, the lighting unit, the irrigation network, and the control unit (Figure 1). The thermally insulated acclimatization chamber had external dimensions of 114 cm in length, 74 cm in width, and 202 cm in height.

A 3 cm square stainless-steel tube was used to build the chamber structure, which was then welded together. All walls were insulated with 2 cm thick high-density foam placed between two sheets of high quality 304 L stainless steel that were 0.15 cm thick to reduce heat transfer. High-density foam layered between two 4 mm thick and 1 cm thick glass plates served as insulation for the chamber door as well. The acclimatization chamber has a working size of 110 cm × 70 cm and 192 cm. The total number of plants was forty-eight, each shelf accommodating twelve plants and there were four shelves (each measuring 100 cm by 50 cm). Transparent 4 mm thick glass panels were used to make the shelves.

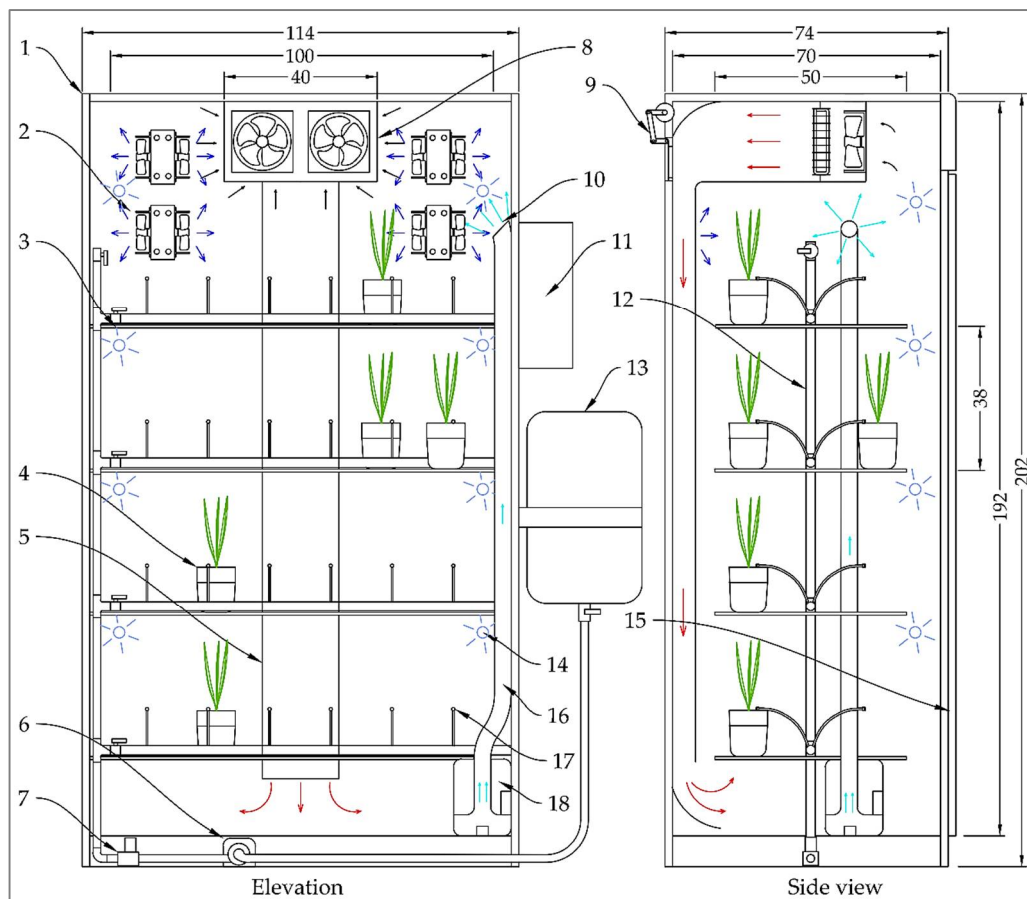


Figure 1. The elevation and side view of the ex vitro acclimatization system (E-VAS) components, all dimensions in centimeters. (1) The frame of the acclimatization chamber, (2) cooling unit (total number of cooling units was four), (3) plantlets shelves (total number of shelves was four), (4) plantlets pot (total number of pots was 48), (5) hot air duct, (6) water pump, (7) water solenoid valve, (8) heating unit, (9) ventilation gate, (10) outputted mist, (11) control unit, (12) main irrigation pipe, (13) water tank, (14) compact fluorescent light (CFL) bulb (total number of CFL bulbs was eight), (15) chamber door, (16) mist duct, (17) dripper (total number of drippers was 48), (18) ultrasonic humidifier.

The acclimatization chamber had a working size of 110 cm × 70 cm and 192 cm. It contained four shelves (100 cm × 50 cm), each accommodating 12 plants, and the total number of plants was forty-eight. The shelves were made of 4 mm thick transparent glass panels.

The E-VAS was equipped with heating, cooling, and humidification units to modify the interior microclimate at the targeted temperature and RH. The heating unit consisted of a 220 V electrical heater with a power of 1000 W and two 220 electrical fans with a diameter of 10 cm. Four cooling units were used to cool the acclimatization chamber when needed. Each cooling unit consisted of a 12 V solid-state refrigerator (Peltier cooler) with a size of 5 × 5 × 0.39 cm and a maximum power of 90 W, an aluminum heat sink with

two 12 V fans for cooling, and two 12 V fans for transferring heat from the hot surface of the Peltier to the outside. The ultrasonic humidifier was used to control the RH inside the chamber [64,65]. This ultrasonic humidifier consisted of one ultrasonic transducer, the water reservoir, the air fan, and the mist duct. The ultrasonic transducer (2600 kHz) was seated at the central bottom position of the reservoir. The E-VAS was supplied with eight compact fluorescent light (CFL) bulbs (220 V, 65 W 6500 K, CFL, OSRAM GmbH, Munich, Germany) with 400–500 nm wavelength. The CFL has a compact electronic ballast inside the bulb base. Two (CFL) bulbs were installed above each shelf to ensure light distribution. The irrigation network included a water tank with 30 L capacity connected to the water source, a water pump with a maximum output of 1.8 L min^{-1} (Model: LF-30LN, Hidro Water S.L.U, Aldaia, Spain), manual valves, a pressure regulator with pressure gauge, solenoid valve, water filter, the irrigation pipes, and the adjustable mini drippers (WS-OCTA-8T, Alwasail Industrial Co., Riyad, Saudi Arabia). High-density polyethylene pipes were used to assemble the irrigation network, including the mainline (20 mm diameter), sub-mainline (15 mm diameter), and feeder pipe (5 mm diameter). The water filter was used to filter the water to prevent any impurities. The control panel consisted of the power source, controllers, Wi-Fi module, fuse, LED indicator, and electrical switches.

2.2. Description of the IoT-Based Monitoring and Control System

The smart IoT-based designed system was aimed to manage the E-VAS by employing the efficient capabilities of cloud computing and the IoT for monitoring the most important environmental parameters, i.e., temperature, RH, air quality, and the light intensity within the E-VAS chamber and volumetric moisture content and pH of the plantlet potting substrate. The system controlled various parameters in the E-VAS, i.e., the temperature and RH of the air and substrate moisture content, to maintain optimum temperature, RH, and the water needed by the plantlet, and automatically notified the user in an emergency by sending an alert notification. In addition, the IoT-based system monitored the temperature, RH, and light intensity in the TGAS and outdoor temperature and RH.

The IoT-based system acquires real-time data from the sensors, uploads it to the cloud platform of ThingSpeak through the internet, analyses it, makes decisions, and communicates to the E-VAS for execution. Moreover, the user can monitor the targeted parameters through the ThingSpeak platform and the mobile application of ThingSpeak. The detailed communication and workflow among the different components of the designed IoT-based system are shown in Figure 2. The microcontroller in the system makes controlled decisions based on the direct measurement of the temperature sensor for operating the cooling or heating units, measurement of the RH sensor for operating the humidification unit, and measurement of the volumetric moisture content sensor for operating the irrigation valve and water pump. The irrigation control by this system can be considered a sensor-based irrigation scheduling. The system schedules the water amount to be applied to the plantlets at variable periods based on the information received from the soil moisture sensors.

The IoT-based monitoring and control system includes six main parts, i.e., the sensors, microcontroller, an internet source, the cloud-based IoT platform, control devices, and web-based Apps, as shown in Figure 2. These parts were connected and integrated for control and monitoring purposes.

Figure 3 shows the detailed schematic Proteus simulation diagram with the main components of the control and monitoring of the E-VAS. Proteus software (Version 8.11) was used to execute the electronic circuit simulation for all the sensors and electric actuators to confirm the compatibility of these devices in operation. The circuit includes the Wi-Fi module (ESP8266, NodeMCU, Shenzhen Quine Trading Co., Ltd., Shenzhen, China) for internet connectivity and an Arduino UNO microcontroller board (Microchip ATmega328P, Microchip Technology Inc., W Chandler Blvd, Chandler, AZ, USA) for data acquisition from the sensors. It controls the heating, cooling, and irrigation actuators. The sensors include the digital DHT22 temperature and RH sensor (ASAIR Electronic Co., Ltd., Huangpu District, Guangzhou, China), the analog DX-250 pH sensor (Daxin Electronic Technology

Co., Ltd, Dongguan, China), the analog LM35 temperature sensor (Focus Sensing and Control Technology Co., Ltd., Hefei, China), the analog VH400 volumetric soil moisture content sensor (Vegetronix, Inc., Riverton, Salt Lake County, UT, USA), the analog MQ-135 air quality sensor (Ke Zhi You Technology Co., Ltd., Shenzhen, China), and the FUT3101 light intensity sensor module (Ke Zhi You Technology Co., Ltd., Shenzhen, China). The control of the actuators was through four relays, i.e., RL1 for controlling the heating unit, RL2 for controlling the cooling units, RL3 for controlling the ultrasonic humidifier, and RL4 for controlling the water pump and the irrigation valves. The connections among the sensors, microcontrollers, and relays, are shown in Figure 3.

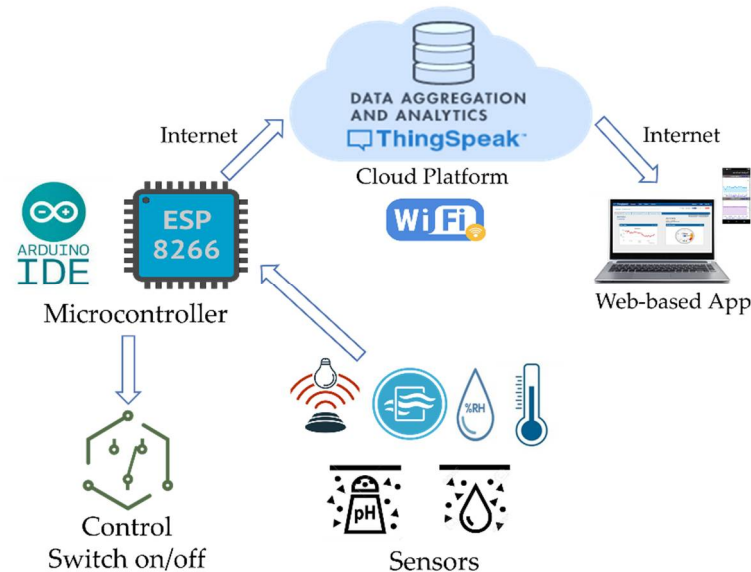


Figure 2. An overview of the IoT-based control and monitoring system for the ex vitro acclimatization system (E-VAS).

2.3. IoT-Based Monitoring, Alerting, and Control Software Layout

In this study, we used Arduino IDE free software repeatedly executed on the Arduino and ESP8266 microcontrollers to monitor and control the targeted parameters in the E-VAS chamber. Mohammed et al. [48,60] describe the detailed functions used in the code. The main function description in the code is as follows: (1) `IntializeSensors()`: This function was responsible for implementing sensors' calibration and resetting them if needed. (2) `GetData()`: The sensor readings were collected every 500 ms and the reading interval was represented using the if condition "if (CurrentTime—LastGetTime >= GetInterval)". Therefore, every 500 ms, the `GetData()` collects the readings from the sensors connected to the microcontroller. The process is performed based on each sensor configuration. (3) `Upload2ThingSpeak()`: This function was used to transmit the collected reading from the sensors to the private cloud channel configured on the ThingSpeak platform. The upload stage was accomplished in real time. (4) `Track()`: This function was considered a local monitoring, showing system activity on the Arduino IDE. The sensors' readings are displayed on the serial monitor. Further, in case of an error, the alert message was shown on the serial monitor to alert the local administrator about the troubling issue. (5) `Print2LCD()`: This function was used to show the readings and alerts on the LCD that connected to the Arduino board. (6) The real-time measurements were uploaded onto the ThingSpeak cloud platform, which was used for data analytics and sending alerts to the administrator.

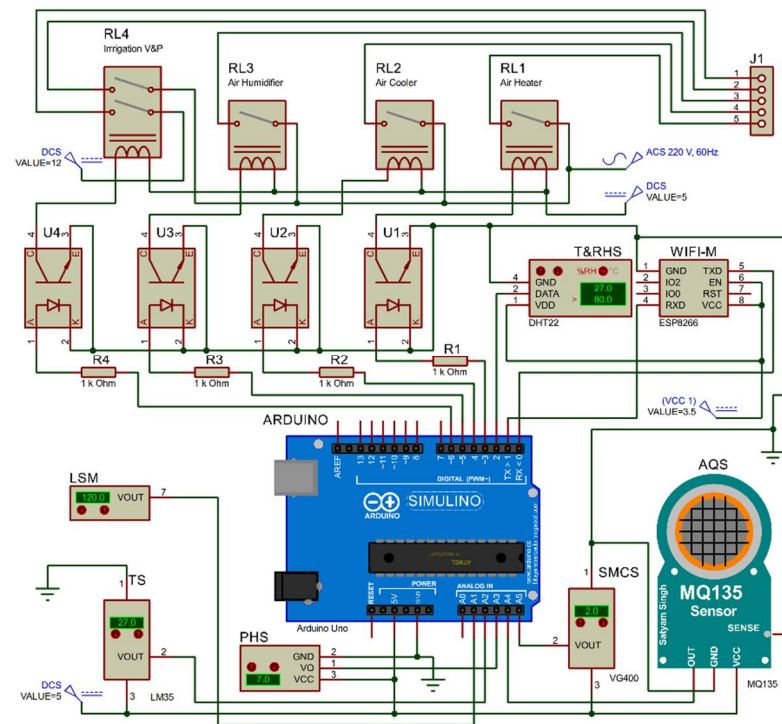


Figure 3. The schematic Proteus simulation diagram with the main components of the control and monitoring of the E-VAS. RL1, RL2, RL3, and RL4 are the relays for the heater, the cooler, the humidifier, and the irrigation control, respectively, U1, U2, U3, and U4 are the optocouplers, R1, R2, R3, and R4 are the 1 k Ohm resistors, ARDUINO is the Arduino UNO microcontroller with ATmega328P Microchip, LSM is the FUT3101 light sensor module, TS is the LM35 temperature sensor, PHS is the DX-250 pH sensor, SMCS is the VH400 volumetric substrate moisture sensor, AQS is the MQ135 air quality sensor, VCC1 is the 3.5 V DC power source, DCS is the DC power source, ACS is the 220 V AC power source, and WIFI-M is the ESP8266 NodeMCU board.

The alerts were conducted using the MATLAB Analysis App on the ThingSpeak platform after configuring the ThingSpeak channel. The MATLAB code was written in the same App for the targeted parameters, i.e., the substrate's temperature, RH, volumetric moisture content, and air quality. The control system of the E-VAS was introduced to control these parameters, as shown in Figure 4. In addition, the alert system of the E-VAS was introduced to alert administrators to minimum light intensity and minimum and maximum values of temperature, RH, and volumetric substrate moisture content, as shown in Figure 5. The alert system sends an email to the administrator through the configured private channel on the ThingSpeak cloud platform.

2.4. Sensor Calibration and Validation

The sensors used in this study, i.e., the digital DHT22 temperature and RH sensor, the analog DX-250 pH sensor, the analog LM35 temperature sensor, the analog VH400 volumetric soil moisture content sensor, the analog MQ-135 air quality sensor, and the FUT3101 light intensity sensor module were calibrated using the same techniques described in previous studies [48,60,66] to ensure their accuracy and are briefly described below:

- The digital DHT22 temperature and RH sensors and the analog LM35 temperature sensor were calibrated by comparing the sensors' readings to the readings of a calibrated incubator (model: PC900h, Helmer Scientific Inc., Noblesville, IN, USA). The incubator temperatures and RH were set at various values, and the observed temperature and RH values were compared with the sensor's readings. Then, the regression equation for each parameter was used to calibrate the used sensors.

- The analog DX-250 pH sensor was calibrated by comparing the sensors' readings to a pH meter's readings (Model HI-99121, Hanna Instruments, Leighton Buzzard, Bedfordshire, UK) at various soil pH values, and the observed pH values were compared with the sensor's readings. Then, the regression equation for the pH was used to calibrate the DX-250 pH sensors.
- The MQ-135 is an air quality sensor for detecting many gases, including CO₂, NH₃, alcohol, and smoke. In this study, the MQ-135 was used to measure the CO₂ concentration (%) in the acclimatization chamber of the E-VAS. To calibrate the MQ-135 sensor, it was heated for 24 h then the reading was acquired. The sensor reading was compared with the reading recorded by a CO₂ device (model: Extech EA80, FLIR Commercial Systems Inc., Nashua, NH, USA) at 25 °C in the closed incubator. The concentration of CO₂ in the incubator was changed using a carbon dioxide cylinder containing 99.5% CO₂. The CO₂ concentration in the incubator was set at various values, and the observed CO₂ values were compared with the sensor's readings. Then, the regression equation for CO₂ was used to calibrate the used MQ-135 sensor for detecting CO₂ in the acclimatization chamber of the E-VAS.
- The VH400 volumetric soil moisture content sensor is a professional electronic sensor. This sensor was selected due to multiple advantages, i.e., it has high sensitivity, is waterproof and rugged, and it can ignore the soil's salt. Moreover, the VH400 sensor is very thin; thus, the probe does not damage the roots of the plantlets and it suits our real-time measurements. The output voltage of this sensor is proportional to the medium moisture content. The VH400 sensor was calibrated by comparing its reading with the actual volumetric moisture content of the medium. It was determined by drying the medium sample of 100 g at 105 °C under a vacuum for 48 h using a vacuum-drying oven (LVO-2041P, Daihan Labtech Co., Ltd., Namyangju-si, Gyeonggi-do, Korea).
- To calibrate the light intensity sensor module, the reading of the module was compared with the reading acquired by the light intensity datalogger (model: Extech EA33, FLIR Commercial Systems Inc., Nashua, NH, USA). First, the calibration was conducted using a compact fluorescent light bulb in the acclimatization chamber with variable illumination intensity at a temperature of 27 °C. Then, the regression equation for light intensity was used to calibrate the sensor for detecting the light intensity in the acclimatization chamber of the E-VAS.

2.5. Experimental Setup

To validate the performance of E-VAS for the improvement of the plants' survival rate and their morpho-physiological characteristics, we set up this experiment to compare the E-VAS (Figure 6) with the TGAS (Figure 7). Tissue culture-derived plantlets transferred to E-VAS were exposed to 27 ± 1 °C temperature, $80 \pm 5\%$ RH, and $600 \mu\text{mol m}^{-2} \text{s}^{-1}$ light intensity for the first 6 weeks. From week 7 onwards, the required temperature, RH, and light intensity were 30 ± 1 °C, $50 \pm 5\%$, and $800 \mu\text{mol m}^{-2} \text{s}^{-1}$, respectively [67]. Therefore, in the first six weeks, the minimum temperature and RH were set at 26.5 °C and 78%, respectively, while the maximum temperature and RH were set at 27.5 °C and 82%. After the six weeks, the minimum temperature and RH were set at 29.5 °C and 48%, respectively, while the maximum temperature and RH were set at 30.5 °C and 52%, respectively. The lighting time was controlled at the targeted light intensity using a 220 V programmable timer switch (Model: CN101, Wenzhou Weilan Electric Co., Ltd., Yueqing, China). The plantlets in the E-VAS plants were irrigated automatically from the first week to the end of the experiment by a sensor-based scheduling method using the H400 soil moisture sensor and the electronic control system. The minimum moisture content of the medium was set at 25%, and the maximum moisture content was set at 40%. Figure 6 shows the experimental setup of the tissue culture plantlets' (TCPs) acclimatization in the E-VAS chamber.

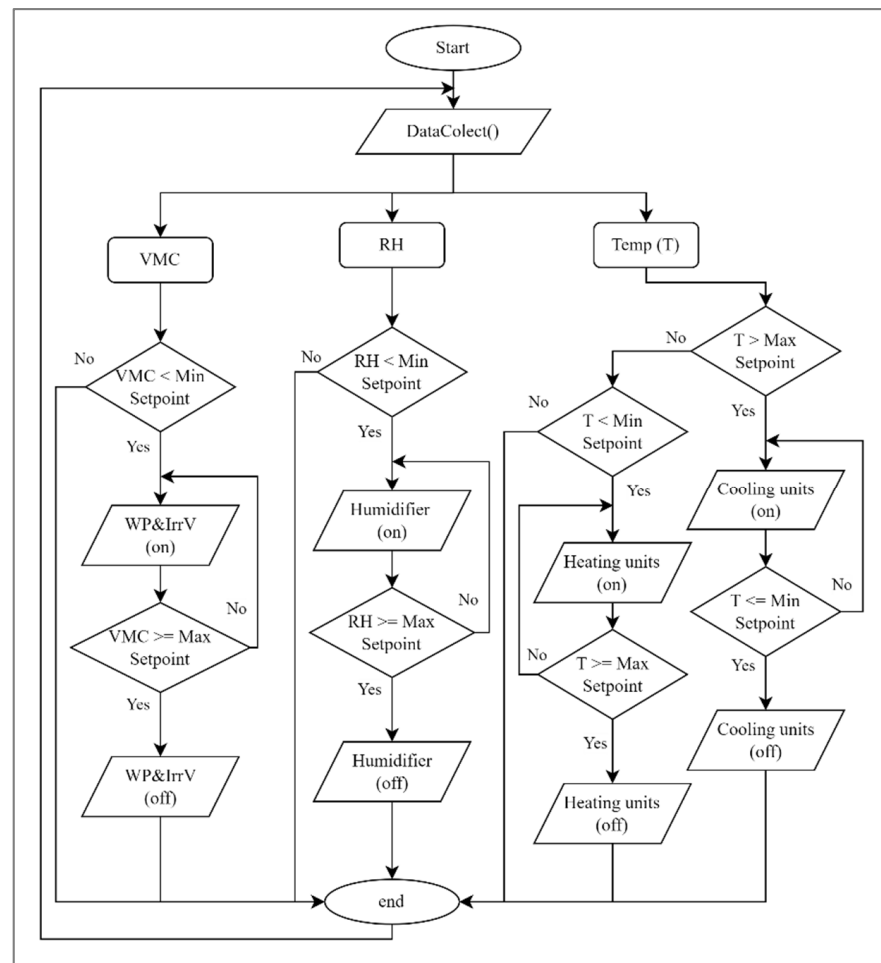


Figure 4. The control flowchart for the E-VAS chamber. Temp (T) is the chamber temperature, RH is the chamber relative humidity, VMC is the volumetric moisture content of the substrate, WP is the water pump, and IrrV is the irrigation solenoid valves.

The plantlets transferred to the TGAS were kept in a white polyethylene compartment for ten days, where high humidity (85–90%) was provided by misting. After ten days, plantlets were uncovered for 15 min for ventilation. This procedure was carried on for two months, and the polyethylene cover was removed [40]. The minimum temperature in the glasshouse was set at 26.5 °C, and the maximum temperature was set at 27.5 °C for the first six weeks. From week seven onwards, the minimum temperature was set at 29.5 °C, and the maximum temperature was set at 30.5 °C. The glasshouse has temperature control and lighting systems to control the minimum light intensity. The lighting time was controlled at the targeted light intensity using a 220 V programmable timer switch (CN101). The plantlets in the TGAS were irrigated automatically every day from the first week to the end of the experiment by a time-based scheduling method using a digital irrigation timer (Model: HT1084, Ningbo Ecowis Plastic & Electric Co., Ltd., Ningbo, China). The operating time of the irrigation timer was determined based on experimental measurements to apply the required water amount to the plantlets. The irrigation network, i.e., irrigation pipe length and diameter and dripper type in the TGAS, were similar to the irrigation network used in the E-VAS. Figure 7 shows the experimental setup of the TCPs' acclimatization in the TGAS.

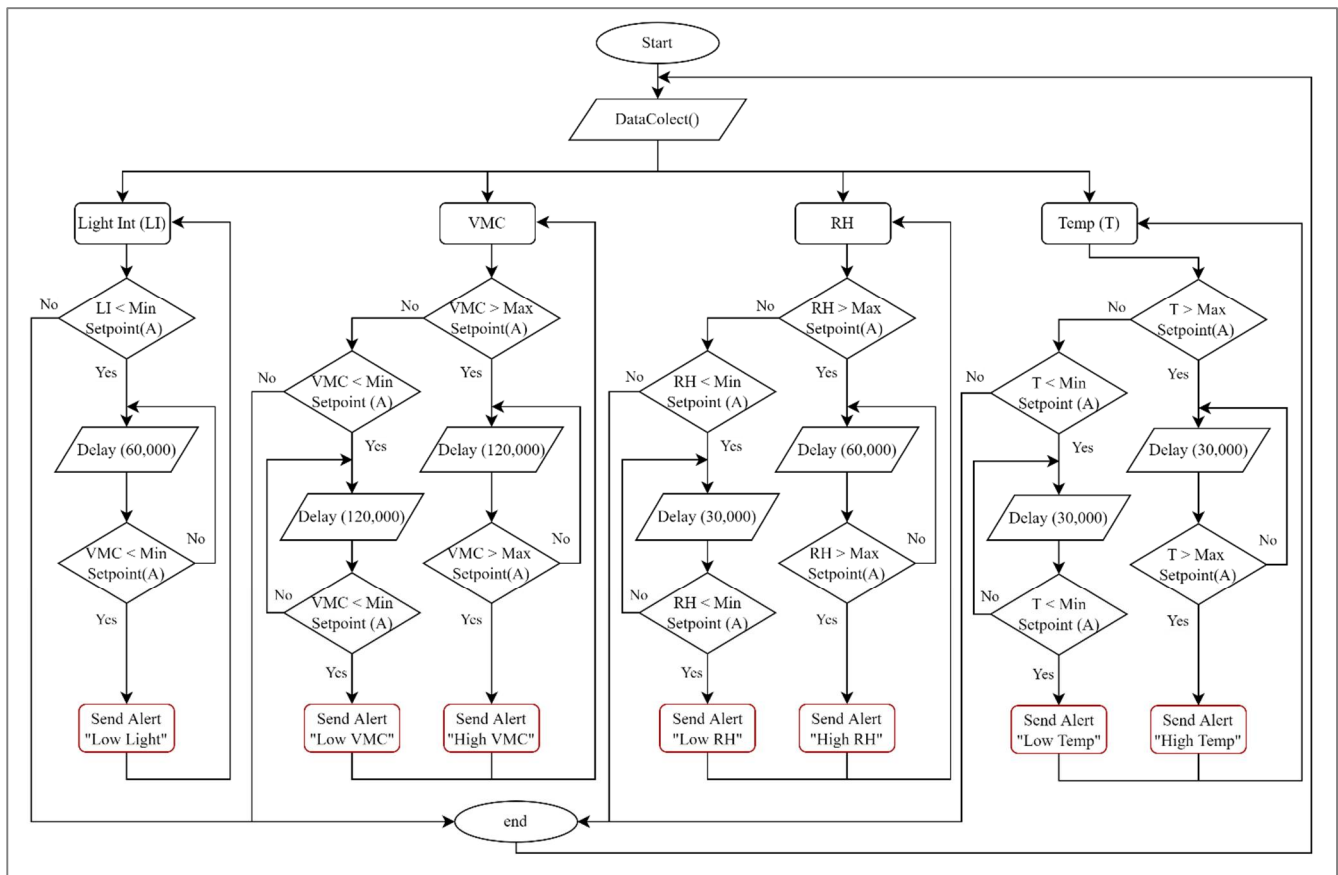


Figure 5. The alert flowchart for the E-VAS chamber. Temp (T) is the chamber temperature, RH is the chamber relative humidity, VMC is the volumetric moisture content of the substrate, Light Int (LI) is the light intensity, and Setpoint (A) is the alert setpoint.

2.6. Tissue Culture-Derived Plant Material

The department of Date Palm Biotechnology, Date Palm Research Center of Excellence, King Faisal University, Saudi Arabia, supplied plantlets of date palm cv. Khalas. These plantlets were produced through the *in vitro* meristem culture technique using the direct organogenesis method, which has both leaf and roots in the test tubes. Plantlets were incubated under cool white fluorescent tubes ($30 \mu\text{mol m}^{-2} \text{s}^{-1}$) inside the growth room of the tissue culture laboratory, where an automatic timer maintained a 16 h photoperiod. The tissue culture growth room temperature was maintained at $24 \pm 2 \text{ }^\circ\text{C}$ during somatic embryo germination, while at the organogenesis phase (rooting and elongation stage), the temperature was increased up to $27 \pm 2 \text{ }^\circ\text{C}$. Before moving the TCPs inside the E-VAS and the TGAS, the plantlets with well-developed roots and leaves underwent pre-acclimatization. Then, the plantlets were transferred to a liquid medium free from plant growth regulators and having a small amount of sucrose. For the gaseous exchange inside and outside the culture tubes, a hole was created in the aluminum foil of each test tube [68]. Plantlets in these test tubes were left for eight hours to undergo *in vitro* hardening. Before transplantation, the roots of plantlets were thoroughly washed with tap water to remove agar gel. Additionally, the plantlets were submerged in a 3 g L^{-1} fungicide solution for up to five minutes before being placed in pots [40].

Ninety-six uniform, healthy, randomly selected test tube plantlets were divided into two groups (E-VAS and TGAS); each group contained forty-eight plantlets. To prevent fungal infection, all plantlets were sprayed with a solution of copper oxychloride.

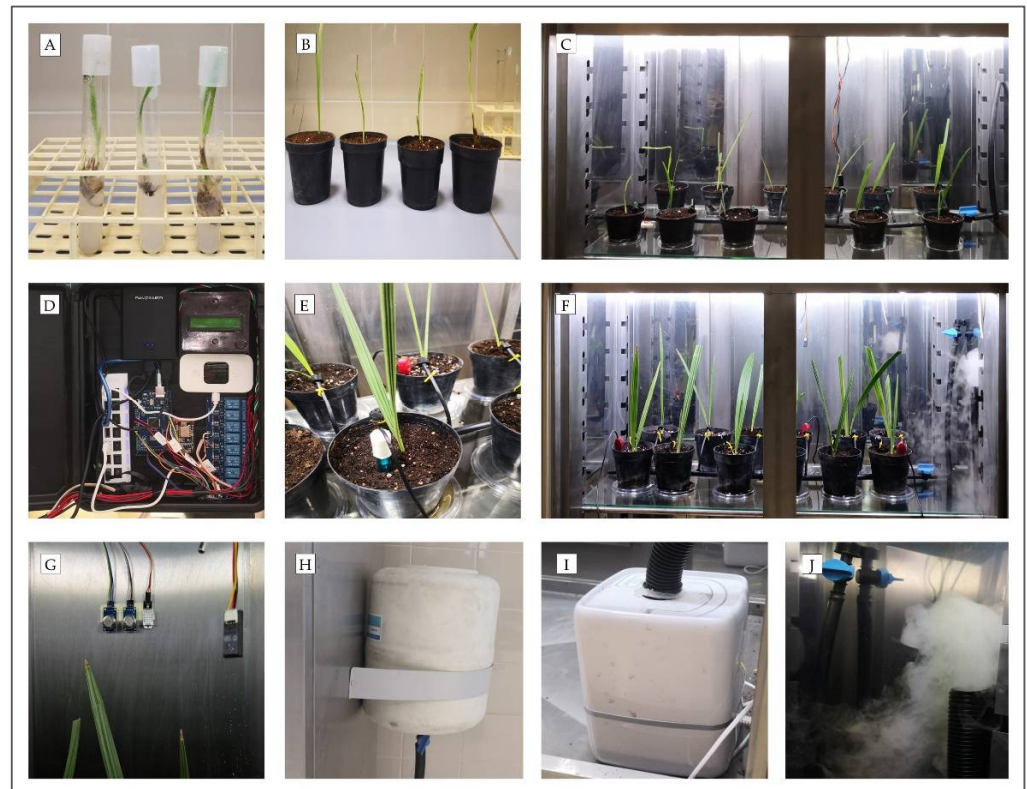


Figure 6. The experimental setup of TCPs for acclimatization in the E-VAS chamber. (A) In vitro plantlets, (B) *Ex vitro* plantlets, (C) Plants after the first week of transfer into the E-VAS chamber, (D) Hardware for monitoring and controlling the automated system, (E) Soil moisture content and soil pH sensors, (F) Plantlets after six months, (G) RH, temperature, and air quality sensors, (H) Water tank, (I) The ultrasonic humidifier, and (J) Outputted mist.



Figure 7. The experimental setup of TCPs for acclimatization in the TGAS. (A) Screenshot from Google of the glasshouse site, (B) The experimental setup, (C) Air conditioning and lighting systems in the glasshouse.

2.7. Potting Media and Cultural Practices

The plantlets were transplanted into pots with a diameter of 6 cm (280 cm³) for the first 6 weeks and thereafter into pots with a diameter of 10 (1200 cm³). The potting

media contained a mixture of 50% sandy loam soil, 40% peat moss compost, and 10% perlite. The sandy loam soil was air-dried at room temperature, sieved through 2 mm stainless steel mesh, and sterilized in the autoclave at 121 °C for 2 h. The analysis of sandy loam soil showed that it contained 76.47% sand, 8.89% silt, 14.64% clay, 7.74 pH, 3.64 dS m⁻¹ EC, 3.38% moisture content, 1.59 g cm⁻³ bulk density, 0.26% organic matter, 16.47 mg kg⁻¹ total nitrogen, 11.72 mg kg⁻¹ phosphorus, and 14.31 mg kg⁻¹ potassium. The peat moss compost had 5.18 pH, 2.51 dS m⁻¹ EC, 41.33% moisture content, 0.88 g cm⁻³ bulk density, 90.84% organic matter, 958 mg kg⁻¹ total nitrogen, 355 mg kg⁻¹ phosphorus, and 561 mg kg⁻¹ potassium.

The time-based scheduling was applied daily to irrigate the plantlets in TGAS, while the sensor-based scheduling was applied to irrigate the E-VAS plants. Weeds were manually removed at emergence. All plants were fertilized equally with the N: P: K ratio of 08—04—14 at different intervals in the TGAS and E-VAS. The plants were rotated once per fortnight interval to prevent errors caused by potential changes in growth conditions in the TGAS.

2.8. Measurements of Morphological Parameters

Data regarding plant height, rhizome size, root length, root number, leaf number, total leaf area, shoot fresh and dry weight, root fresh and dry weight, root shoot fresh and dry weight ratio, and total biomass, were recorded at test tube plantlet stage, after 6 and 12 months under acclimatization stages. Plant height and root length were calculated using a measuring tape. Root and leaf numbers were counted visually. Vernier slide caliper was used to measure rhizome size. The leaf area was estimated using a portable leaf area meter (CI-202, CID Bio-Science, Camas, WA, USA). Dry weights, leaf fresh weight, and root fresh and dry weights were also measured by Sartorius electronic balance (Sartorius Lab Instruments GmbH & Co., Göttingen, Lower Saxony, Germany). To determine the leaf and root dry weight, they were washed with tap water, dried at room temperature, and then placed in an oven (BINDER™ Series E Classic, Fisher Scientific, Waltham, MA, USA) to constant weight at 70 °C for 72 h. After each month, the percentage of plant mortality in both environmental compartments was recorded. The percentage of plant mortality of tissue culture-derived date palm (cv. Khalas) plants under the designed ex vitro acclimatization system (E-VAS) and traditional greenhouse acclimatization system (TGAS) was calculated after one month period until six months using following equation:

$$\text{Mortality (\%)} = \frac{\text{Number of dead plants}}{\text{Total number of plants}} \times 100$$

2.9. Estimation of Physiological Parameters

Physiological parameters such as chlorophyll content, photosynthesis, stomatal conductance, transpiration rate, and intercellular CO₂ concentration were recorded at test tube plantlets stage, after 6 and 12 months under the acclimatization stages. The leaf chlorophyll content was calculated using a chlorophyll meter (SPAD 502, Konica–Minolta Inc., Tokyo, Japan). The photosynthesis, stomatal conductance, transpiration rate, and intercellular CO₂ concentration were determined using the Li-6400XT photosynthesis system (LiCor Inc., Lincoln, NE, USA) as described previously [69]. The leaf was inserted in the Infra-Red Gas Analyzer (IRGA) chamber to estimate photosynthesis and related parameters. The leaf temperature of the IRGA chamber was adjusted at 30 °C. Inside the chamber, both reference and sample CO₂ were set at 400 μmol m⁻² s⁻¹ with 500 μmol s⁻¹ airflow.

2.10. Statistical Analysis

The data sample was comprised of ten plants for each parameter studied. The recorded data were used to calculate treatment mean values and standard deviation within replicates. The data were analyzed using Genstat software, version 11 (VSNi International Ltd., Hemel Hempstead, UK). A two-factorial completely randomized design (CRD) was used for the analysis of variance (ANOVA) test. Two different environment conditions (E-VAS

and TGAS) were taken as factor one and the plant ages (TTP, 6MOP, and 12MOP) were considered as factor two. There was a complete sapling randomization between the two factors. As a fixed effect factor, the E-VAS and TGAS environmental conditions were selected since they have an impact on plants of various ages (TTP, 6MOP, and 12MOP) as they acclimate. For multiple comparisons of means, the least significant difference (LSD) test was used to find out statistical significant difference among treatment means at 5% level of probability ($p < 0.05$).

The temperature, RH and light intensity data of outdoor, indoor, TGAS, and E-VAS conditions were recorded by the sensors after every 5 s for a 12 month period. These environmental variables were analyzed separately on monthly basis using one-way ANOVA method of Genstat computer program. To analyze plant mortality data, paired Student t-test was applied on mean observations of the respective parameter.

Linear regression was used to obtain calibration formulas for all used sensors, i.e., DHT22 digital temperature and RH sensors, DX-250 analog pH sensor, LM35 analog temperature, VH400 volumetric soil moisture content sensor, MQ135 air quality sensor, FUT3101 light intensity sensor. The following equation expresses the linear regression:

$$y = \beta_0 + \beta_1x + \beta_2x^2 + \dots + \beta_nx^n + \varepsilon \quad (1)$$

where y is the dependent variable (response), x is the response-independent variable, β_0 is the constant of the y -intercept, β_1 , β_2 , and β_n are the constants of the slope coefficients for the explanatory variable, n is the multiple linear regression equation degree, and ε is the random error variable.

Simple linear regression ($y = \beta_0 + \beta_1x$) was used to determine the relationship between the sensor measurements (dependent variable) and the observed values (independent variable) after sensor calibration. In addition, the most important evaluation criteria, i.e., the Coefficient of Determination (R^2), the Mean Absolute Percentage Error (MAPE), and the Root Mean Square Error (RMSE) values [60,70], were used to validate the performance of the sensor before using them. The Coefficient of Determination assesses the strong linear relationship between the observed and measured values measured by the standard instrument. The Mean Absolute Percentage Error is the average of absolute errors divided by the actual observed values. The Mean Absolute Percentage Error should not be used if any value in the actual data equals zeros or near-zeros. Mean Square Error depicts the mean squared difference between the observed and the measured values. The RMSE compares the difference between the observed and measured values by the sensor. An R^2 value closer to 1 and MAPE and RMSE values closer to 0 exhibit more agreement between the observed and the measured values. The R^2 values are closely related to the MAPE and RMSE values. The following equations express the R^2 , MAPE, and RMSE:

$$R^2 = 1 - \frac{SS_{\text{res}}}{SS_{\text{tot}}} = 1 - \frac{\sum (Y_i - \hat{Y})^2}{\sum (Y_i - \bar{Y})^2} \quad (2)$$

$$\text{MAPE} = \frac{\sum_{i=1}^n \left| \frac{Y_i - \hat{Y}}{Y_i} \right|}{n} \times 100 \quad (3)$$

$$\text{RMSE} = \sqrt{\frac{\sum_{i=1}^n (Y_i - \hat{Y})^2}{n}} \quad (4)$$

where SS_{res} is the residual sum of squares, SS_{tot} is the total sum of squares, Y_i is the observed value, \hat{Y} is the measured value, \bar{Y} is the mean of actual values, and n is the number of measurements.

3. Results

3.1. System Validation

3.1.1. Sensors

To assure the accuracy of the measurements in this investigation, all the used sensors underwent calibration and validation prior to the experiment. Table 1 illustrates the evaluation criteria values, i.e., R^2 , MAPE, and RMSE, and linear regression equations for the digital DHT22 temperature and RH sensors, analog DX-250 pH sensor, the analog LM35 temperature sensor, the analog VH400 volumetric soil moisture content sensor, the analog MQ-135 air quality sensor, and the FUT3101 light intensity sensor module. According to all the evaluation criteria (R^2 , MAPE, and RMSE) and the linear regressions models that almost overlapped the 1:1 line ($y = x + 0$), all the sensors performed well, indicating a perfect match between the measured temperature, RH, light intensity, pH, air quality, and volumetric soil moisture content and their observed values.

Table 1. Validation of the digital DHT22 temperature sensor (DTS), RH sensor (RHS), analog DX-250 pH sensor (pHS), analog LM35 temperature sensor (ATS), analog VH400 volumetric soil moisture content sensor (VMCS), analog MQ-135 air quality sensor (AQS), and FUT3101 light intensity sensor (LIS).

Sensors	Min-Max Values	n	Evaluation Criteria			LRE
			R^2	MAPE	RMSE	
DTS	1–50 °C	200	0.976	8.613	1.668	$y = 0.991x - 0.652$
RHS	10–90%	200	0.966	10.462	4.375	$y = 1.014x + 2.078$
pHS	5–8	20	0.948	3.516	0.290	$y = 0.973x + 0.003$
ATS	1–50 °C	200	0.994	4.303	0.834	$y = 0.997x - 0.326$
VMCS	22–40%	20	0.968	1.991	0.894	$y = 1.006x - 0.075$
AQS	0.04–0.4%	30	0.994	9.804	0.011	$y = 0.983x - 0.001$
LIS	10–890 $\mu\text{mol m}^{-2} \text{s}^{-1}$	50	0.995	7.547	22.761	$y = 11.65x + 1.505$

In the above table, Min-Max values, n, R^2 , MAPE, RMSE, and LRE represent the minimum and maximum values of measurement of each sensor, number of measurements, Coefficient of Determination, Mean Absolute Percentage Error, Root Mean Square Error values, and Linear Regression Equation, respectively.

3.1.2. IoT-Based Monitoring and Control System

The IoT-based system was installed with the objective of controlling and monitoring the actuators and microclimate of the E-VAS in real-time. As a result, the E-heating, VAS cooling, ultrasonic humidifier, irrigation water pump, and irrigation solenoid valve were all turned ON and OFF in accordance with the control system's output signal. However, these fluctuations shorten the life of the relays or adversely affect the irrigation valves, cooling and heating fans and pumps connected to the controller since the output signal changes often in accordance with the sensor data. Hysteresis bands were created between the ON and OFF processes to control this issue and safeguard the relays and E-VAS actuators. Our real-time investigations showed that the E-VAS could be efficiently regulated by adjusting the minimum and maximum setpoints for the substrate's temperature, RH, and moisture content.

Furthermore, the open-source ThingSpeak platform was used to process the real-time measurements of temperature, RH, light intensity, CO_2 , and the substrate's pH and volumetric moisture content [71]. After the private channel was set up and the system was connected to it for the purpose of monitoring the target parameters, Figure 8 shows a screenshot of some real-time measurement data on the ThingSpeak platform. The measurement information for the target parameters was also kept in the cloud as Google spreadsheets, which the administrator utilized to analyze and view the values. Therefore, the user can remotely monitor the E-VAS and access the relevant data of the acclimatization chamber microclimate using the IoT-based monitoring and control system to decide the appropriate actions depending on the current condition.

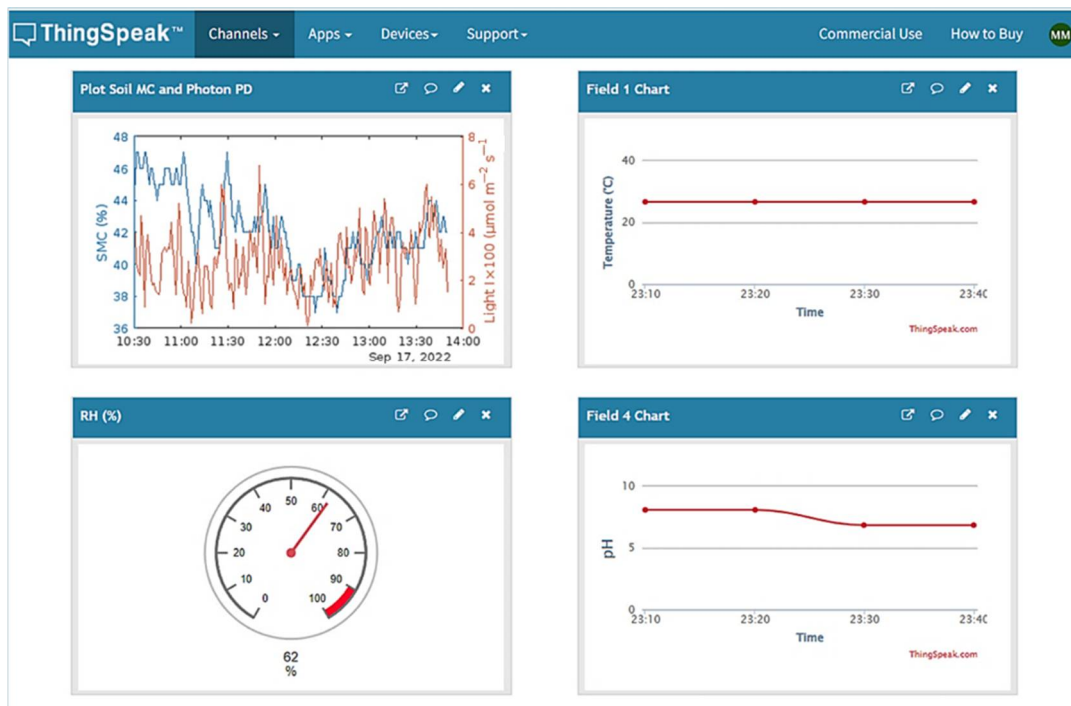


Figure 8. A screenshot of the received soil moisture content (SMC), light intensity (LightI), temperature, RH, and soil pH via the ThingSpeak platform [71].

Figure 9 displays the real-time average temperature readings for the indoor, outdoor, E-VAS, and TGAS environments that were obtained from the DHT22 sensors using the IoT-based system from 1 February 2021 to 31 January 2022. The outdoor temperature ranged from 8.42 to 45.18 °C, with an average of 30.45 ± 9.43 °C. Temperatures indoors ranged from 15.6 to 37.54 °C, with an average of 27.12 ± 6.36 °C. The average TGAS temperature was 30.18 ± 1.06 °C and ranged from 25.39 to 31.92 °C, whereas the average E-VAS temperature was 29.91 ± 0.77 °C, which ranged from 26.55 to 31.1 °C. The temperature variance in the designed E-VAS system was slightly lower than the TGAS. As shown in the flowchart (Figure 4), the IoT-based system with the LM35 temperature sensor was used to control the E-VAS temperature, while the control system was used to regulate the TGAS temperature. In the first six weeks of the study, the minimum and maximum temperature setpoints for the E-VAS and TGAS were both set at 26.5 °C. Afterwards, the minimum and maximum setpoints were set at 29.5 and 30.5 °C, respectively. Afterward, the temperature in the E-VAS did not reach the maximum (35 °C) and minimum (25 °C) alarm setpoints for 30 min, as stated in the flowchart; the IoT-based system did not send any alert notifications during the course of this experiment (Figure 5).

The average RH readings for the outdoor, E-VAS, and TGAS sensors using the IoT-based system are shown in Figure 10 for the period from 1 February 2021 to 31 January 2022. While the RH of the TGAS was not controlled, it was controlled for the E-VAS chamber according to the flowchart (Figure 4). The outdoor, TGAS, and EVAS had significantly different relative humidity levels. In the first six weeks, the RH for the E-VAS was set at 78% as the minimum and 82% as the maximum. Thereafter, it was set at a minimum of 48% and a maximum of 52%. The outdoor RH ranged from 8.63 to 83.72%, with an average of 37.64 ± 5.76 % and the range of the TGAS RH was 36.21 to 58.67%, with an average of 45.76 ± 5.05 %. The average E-VAS RH was 51.22 ± 8.57 % and ranged from 45.24 to 78.77%. Because the RH in the E-VAS reached the highest alert setpoint (60%) for 60 min throughout the experiment, the designed IoT-based system delivered three alert signals (Figure 5). In contrast, the IoT-based system did not send a low RH alert because the chamber's RH remained above the minimum alert setpoint (40%) for 30 min. The IoT-based system and ultrasonic humidifier effectively managed the RH of the E-VAS, delivered alert notifications

depending on the alert setpoints, and attained the targeted RH (Figure 10). Comparing the RH of the TGAS to the E-VAS chamber, a significant variation is observed.

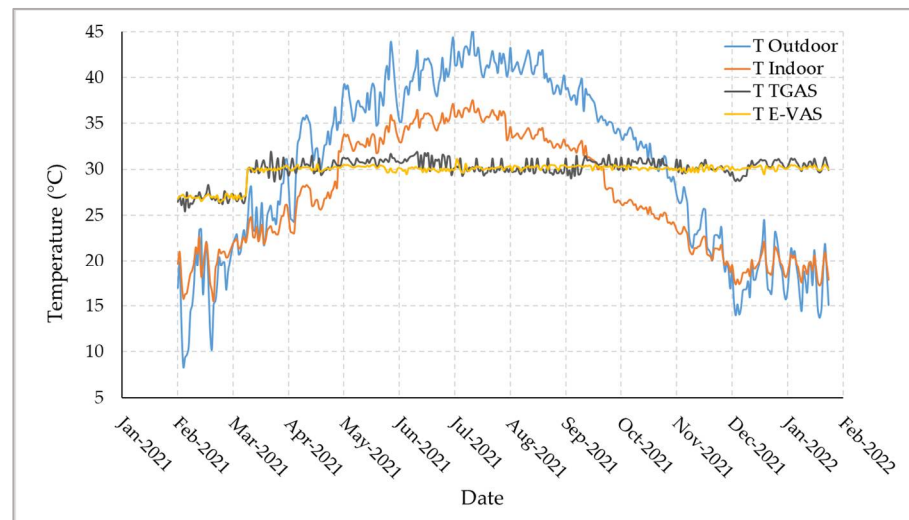


Figure 9. Average temperatures of the outdoor (T Outdoor), the indoor (T Indoor), the traditional greenhouse acclimatization system (TGAS), and the designed ex vitro acclimatization system (E-VAS).

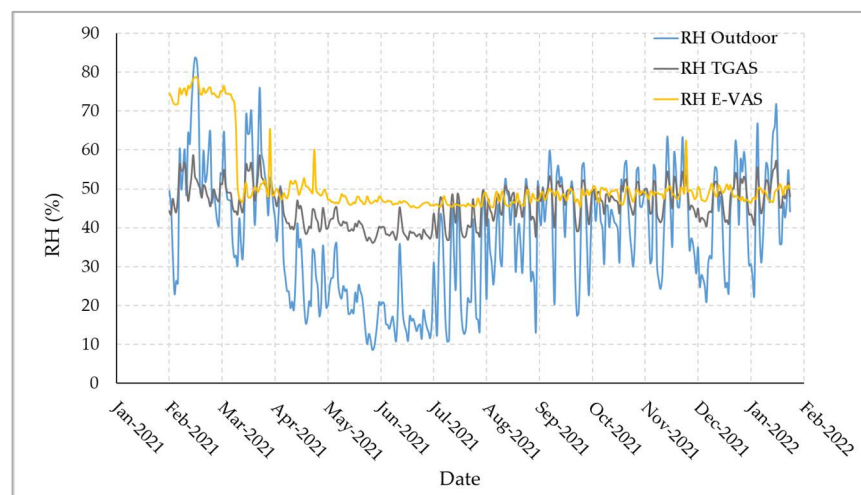


Figure 10. Average RH of the outdoor (T Outdoor), the traditional greenhouse acclimatization system (TGAS), and the designed ex vitro acclimatization system (A-VAS).

Comparing the TGAS and the E-VAS systems, there was a non-significant difference in the environmental variable of light intensity. The light intensity in the E-VAS did not drop below the minimal alarm setpoint ($700 \mu\text{mol m}^{-2} \text{s}^{-1}$) for 60 min; hence, the IoT-based system did not issue any alerts regarding the light intensity during the experiment.

3.2. Morpho-Physiological Attributes

The morphological data presented in Table 2 show that plants acclimatized to the E-VAS environment had significantly greater plant height, rhizome size, root length, leaf number, and total leaf area than plants acclimatized to the TGAS environment. Comparing plant ages, it was observed that the older plants (12 months) had significantly greater plant heights, rhizome sizes, root lengths, leaf number, and total leaf areas. The interaction data of both factors indicated that plants acclimatized under the E-VAS environment performed significantly better after 6 and 12 months regarding plant height, rhizome size, root length, root number, leaf number, and total leaf area parameters compared to the same-aged plants under TGAS environment.

Table 2. Morphological response of different-aged tissue culture-derived date palm (cv. Khalas) plants under ex vitro acclimatization system (E-VAS) and traditional glasshouse acclimatization system (TGAS) environment for acclimatization.

Parameters	Plant Height (cm)	Rhizome Size (mm)	Root Length (cm)	Root Number	Leaf Number	Total Leaf Area (cm ²)
A. Environment						
E-VAS	28.38 ± 1.99 ^a	14.10 ± 0.93 ^a	10.75 ± 1.23 ^a	2.73 ± 0.48 ^a	3.33 ± 0.30 ^a	47.27 ± 3.56 ^a
TGAS	24.90 ± 2.18 ^b	12.36 ± 1.08 ^b	8.84 ± 0.95 ^b	2.47 ± 0.33 ^a	2.87 ± 0.18 ^b	43.11 ± 3.58 ^b
LSD($p \leq 0.05$)	1.70 [*]	0.87 [*]	0.92	0.39 ^{NS}	0.26 [*]	2.95 [*]
B. Plant age						
TTP	13.58 ± 0.69 ^c	6.11 ± 0.53 ^c	5.51 ± 0.39 ^c	1.00 ± 0.00 ^c	2.00 ± 0.00 ^c	25.36 ± 1.60 ^c
6MOP	23.82 ± 3.47 ^b	12.93 ± 0.81 ^b	9.23 ± 1.33 ^b	2.00 ± 0.45 ^b	2.90 ± 0.50 ^b	39.89 ± 4.01 ^b
12MOP	42.52 ± 2.10 ^a	20.65 ± 1.69 ^a	14.64 ± 1.54 ^a	4.80 ± 0.77 ^a	4.40 ± 0.22 ^a	70.33 ± 5.10 ^a
LSD($p \leq 0.05$)	2.08 [*]	1.07 [*]	1.12 [*]	0.47 [*]	0.31 [*]	3.61 [*]
C. Interaction						
E-VAS × TTP	13.50 ± 0.69 ^e	6.00 ± 0.70 ^d	5.41 ± 0.32 ^e	1.00 ± 0.01 ^c	2.00 ± 0.01 ^e	25.2 ± 2.05 ^e
E-VAS × 6MOP	26.60 ± 3.36 ^c	13.26 ± 0.80 ^c	10.50 ± 1.78 ^c	2.20 ± 0.45 ^b	3.20 ± 0.45 ^c	42.89 ± 3.08 ^c
E-VAS × 12MOP	45.00 ± 1.93 ^a	23.05 ± 1.31 ^a	16.34 ± 1.59 ^a	5.00 ± 1.00 ^a	4.80 ± 0.45 ^a	73.73 ± 5.55 ^a
TGAS × TTP	13.65 ± 0.70 ^e	6.22 ± 0.36 ^d	5.62 ± 0.46 ^e	1.00 ± 0.01 ^c	2.00 ± 0.01 ^e	25.52 ± 1.15 ^e
TGAS × 6MOP	21.02 ± 3.57 ^d	12.60 ± 0.81 ^c	7.96 ± 0.88 ^d	1.80 ± 0.45 ^b	2.60 ± 0.55 ^d	36.89 ± 4.94 ^d
TGAS × 12MOP	40.05 ± 2.27 ^b	18.25 ± 2.07 ^b	12.94 ± 1.49 ^b	4.60 ± 0.55 ^a	4.00 ± 0.01 ^b	66.93 ± 4.65 ^b
LSD($p \leq 0.05$)	2.94 [*]	1.51 [*]	1.59 [*]	0.67 [*]	0.44 [*]	5.10 [*]

TTP, 6MOP, and 12MOP in the above table represent test tube plantlets, 6-month-old plants, and 12-month-old plants, respectively. Different letters within each column (parameter) indicate significant mean differences at $p \leq 0.05$, which are separated according to factors and their interaction. Data are the mean of ten independent biological replicates, whereas \pm data represent the standard deviation within replicates. The statistical analysis is based on a two-factorial completely randomized design. The multiple comparisons of means were performed by the least significance difference (LSD) test, where NS represents the non-significant difference and * shows significant difference within the means at 5% level of probability.

The acclimatized plants in the two testing environments revealed that the E-VAS environment significantly enhanced plant biomass-related attributes such as shoot fresh and dry weight, root fresh and dry weight, root shoot dry weight ratio, and total biomass (Table 3). These parameters, including the root shoot fresh weight ratio, increased linearly with plant age and maximized at the 12 month stage. The interaction of both factors indicated that the plants acclimatized in the E-VAS environment for 12 months had a maximum shoot fresh and dry weight, root fresh and dry weight, root shoot fresh weight ratio, root shoot dry weight ratio, and total biomass.

Although the plants acclimatized in the E-VAS environment had much higher chlorophyll content than under the TGAS environment, the chlorophyll content in each environment was significantly lower in TTP and 6MOP than that in 12MOP (Table 4). Other physiological characteristics such as the rate of photosynthesis, the stomatal conductance, the rate of transpiration, and the concentration of intercellular CO₂ were statistically non-significant in both environments (E-VAS and TGAS). Comparing the response of plant age, other physiological characteristics, besides intercellular CO₂ concentration, dramatically increased with plant age. In contrast to the rate of photosynthesis, the stomatal conductance, and the rate of transpiration, plants' responses to intercellular CO₂ concentration reduced as their age increased. These attributes were highest in 12-month-old plants that had been acclimatized to the E-VAS environment, according to the interaction analysis of these parameters.

Table 3. Plant biomass response of different-aged tissue culture-derived date palm (cv. Khalas) plants under ex vitro acclimatization system (E-VAS) and traditional glasshouse acclimatization system (TGAS) environment for acclimatization.

Parameters	Shoot Fresh Weight (g)	Shoot Dry Weight (g)	Root Fresh Weight (g)	Root Dry Weight (g)	Root Shoot FW Ratio	Root Shoot DW Ratio	Total Biomass (g)
A. Environment							
E-VAS	6.75 ± 0.81 ^a	2.28 ± 0.20 ^a	0.65 ± 0.05 ^a	0.29 ± 0.02 ^a	0.09 ± 0.01 ^a	0.12 ± 0.01 ^a	7.57 ± 0.81 ^a
TGAS	5.35 ± 0.74 ^b	1.91 ± 0.11 ^b	0.54 ± 0.05 ^b	0.19 ± 0.02 ^b	0.09 ± 0.02 ^a	0.10 ± 0.01 ^b	6.02 ± 0.74 ^b
LSD ($p \leq 0.05$)	0.64 [*]	0.12 [*]	0.05 [*]	0.02 [*]	0.01 ^{NS}	0.01 [*]	0.63 [*]
B. Plant age							
TTP	2.97 ± 0.62 ^c	0.91 ± 0.13 ^c	0.22 ± 0.01 ^c	0.09 ± 0.00 ^c	0.07 ± 0.01 ^b	0.10 ± 0.02 ^b	3.40 ± 0.62 ^c
6MOP	5.67 ± 0.25 ^b	1.90 ± 0.10 ^b	0.48 ± 0.07 ^b	0.19 ± 0.01 ^b	0.09 ± 0.01 ^b	0.10 ± 0.01 ^b	6.40 ± 0.25 ^b
12MOP	9.51 ± 1.46 ^a	3.47 ± 0.23 ^a	1.08 ± 0.07 ^a	0.43 ± 0.04 ^a	0.12 ± 0.02 ^a	0.12 ± 0.01 ^a	10.58 ± 1.46 ^a
LSD ($p \leq 0.05$)	0.78 [*]	0.14 [*]	0.06 [*]	0.02 [*]	0.02 [*]	0.01 [*]	0.77 [*]
C. Interaction							
E-VAS × TTP	3.02 ± 0.61 ^e	0.92 ± 0.15 ^e	0.21 ± 0.01 ^e	0.09 ± 0.00 ^e	0.07 ± 0.01 ^c	0.10 ± 0.02 ^b	3.44 ± 0.61 ^e
E-VAS × 6MOP	6.44 ± 0.29 ^c	2.22 ± 0.12 ^c	0.56 ± 0.05 ^c	0.24 ± 0.01 ^c	0.09 ± 0.01 ^{bc}	0.11 ± 0.01 ^b	7.28 ± 0.28 ^c
E-VAS × 12MOP	10.81 ± 1.54 ^a	3.70 ± 0.32 ^a	1.17 ± 0.10 ^a	0.53 ± 0.04 ^a	0.11 ± 0.02 ^{ab}	0.14 ± 0.01 ^a	11.97 ± 1.52 ^a
TGAS × TTP	2.93 ± 0.62 ^e	0.89 ± 0.11 ^e	0.22 ± 0.02 ^e	0.09 ± 0.00 ^e	0.08 ± 0.02 ^c	0.10 ± 0.01 ^b	3.37 ± 0.63 ^e
TGAS × 6MOP	4.91 ± 0.22 ^d	1.59 ± 0.07 ^d	0.40 ± 0.09 ^d	0.14 ± 0.01 ^d	0.08 ± 0.02 ^c	0.09 ± 0.01 ^c	5.51 ± 0.22 ^d
TGAS × 12MOP	8.21 ± 1.39 ^b	3.24 ± 0.14 ^b	0.99 ± 0.03 ^b	0.33 ± 0.04 ^b	0.12 ± 0.02 ^a	0.10 ± 0.02 ^b	9.19 ± 1.39 ^b
LSD ($p \leq 0.05$)	1.11 [*]	0.20 [*]	0.08 [*]	0.03 [*]	0.02 [*]	0.02 [*]	1.08 [*]

TTP, 6MOP, and 12MOP in the above table represent test tube plantlets, 6-month-old plants, and 12-month-old plants, respectively. Different letters within each column (parameter) indicate significant mean differences at $p \leq 0.05$, which are separated according to factors and their interaction. Data are the mean of ten independent biological replicates, whereas \pm data represent the standard deviation within replicates. The statistical analysis is based on a two-factorial completely randomized design. The multiple comparisons of means were performed by the least significance difference (LSD) test, where NS represents the non-significant difference and * shows significant difference within the means at 5% level of probability.

For up to six months throughout the study period, plants that were transferred to the TGAS environment for acclimatization exhibited a statistically significant increase in mortality (Figure 11). Within six months, plants transferred to the TGAS environment had a mortality rate of 40.49%, whereas plants transferred to the E-VAS environment had a mortality rate of only 14.12%. The maximum mortality percentage was recorded during the first month of acclimatization, i.e., 17.53% under TGAS and 6.44% under E-VAS environments, which significantly declined thereafter in both environments.

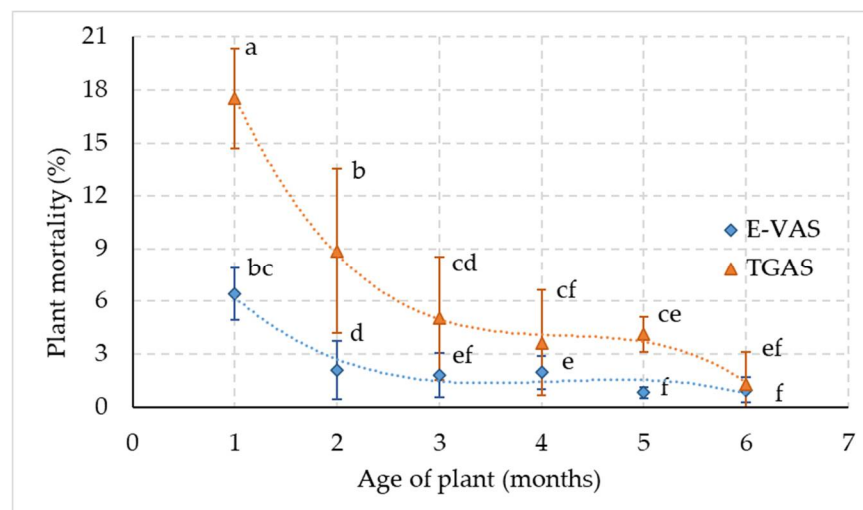


Figure 11. Plant mortality response of tissue culture-derived date palm (cv. Khalas) plants acclimatized under the designed ex vitro acclimatization system (E-VAS) and traditional greenhouse acclimatization system (TGAS) environments. The mortality percentage was calculated after one month period until six months. Y-bars indicate the standard deviation within the sample. Different letters indicate significant differences under E-VAS and TGAS environments. Paired Student t-test was applied on mean data of mortality percentage and the probability value was 0.02.

Table 4. Physiological response of different-aged tissue culture-derived date palm (cv. Khalas) plants under ex vitro acclimatization system (E-VAS) and traditional glasshouse acclimatization system (TGAS) environment for acclimatization.

Parameters	Chlorophyll (SPAD)	Photosynthesis ($\mu\text{mol m}^{-2} \text{s}^{-1}$)	Stomatal Conductance ($\text{mmol m}^{-2} \text{s}^{-1}$)	Transpiration Rate ($\text{mmol m}^{-2} \text{s}^{-1}$)	Inter. CO_2 Conc. ($\mu\text{mol mol}^{-1}$)
A. Environment					
E-VAS	46.05 \pm 2.90 ^a	9.30 \pm 0.81 ^a	17.85 \pm 1.11 ^a	0.52 \pm 0.02 ^a	165.14 \pm 23.36 ^a
TGAS	43.54 \pm 2.16 ^b	8.87 \pm 0.67 ^a	17.38 \pm 0.97 ^a	0.51 \pm 0.03 ^a	174.54 \pm 12.89 ^a
LSD($p \leq 0.05$)	1.97 [*]	0.59 ^{NS}	0.75 ^{NS}	0.02 ^{NS}	12.89 ^{NS}
B. Plant age					
TTP	25.28 \pm 2.18 ^c	7.34 \pm 0.77 ^c	15.98 \pm 0.88 ^c	0.50 \pm 0.02 ^b	211.86 \pm 15.47 ^a
6MOP	51.44 \pm 2.75 ^b	9.24 \pm 0.43 ^b	17.66 \pm 0.96 ^b	0.51 \pm 0.03 ^b	159.28 \pm 20.51 ^b
12MOP	57.66 \pm 2.66 ^a	10.67 \pm 1.03 ^a	19.20 \pm 1.28 ^a	0.55 \pm 0.03 ^a	138.38 \pm 18.40 ^c
LSD($p \leq 0.05$)	2.42 [*]	0.72 [*]	0.92 [*]	0.03 [*]	15.79 [*]
C. Interaction					
E-VAS \times TTP	25.24 \pm 2.86 ^d	7.34 \pm 0.69 ^d	15.99 \pm 0.76 ^d	0.50 \pm 0.02 ^c	212.16 \pm 16.86 ^a
E-VAS \times 6MOP	52.44 \pm 3.05 ^{bc}	9.50 \pm 0.57 ^{bc}	18.06 \pm 1.12 ^{bc}	0.52 \pm 0.03 ^{ac}	152.28 \pm 26.39 ^{bc}
E-VAS \times 12MOP	60.46 \pm 2.78 ^a	11.07 \pm 1.18 ^a	19.50 \pm 1.44 ^a	0.55 \pm 0.03 ^a	130.98 \pm 26.84 ^c
TGAS \times TTP	25.32 \pm 1.50 ^d	7.35 \pm 0.85 ^d	15.98 \pm 1.00 ^d	0.50 \pm 0.03 ^c	211.56 \pm 14.08 ^a
TGAS \times 6MOP	50.44 \pm 2.44 ^c	8.99 \pm 0.29 ^c	17.26 \pm 0.79 ^{cd}	0.51 \pm 0.03 ^{bc}	166.28 \pm 14.64 ^b
TGAS \times 12MOP	54.86 \pm 2.54 ^b	10.27 \pm 0.88 ^{ab}	18.90 \pm 1.13 ^{ab}	0.54 \pm 0.02 ^{ab}	145.78 \pm 9.95 ^{bc}
LSD($p \leq 0.05$)	3.42 [*]	1.02 [*]	1.29 [*]	0.04 [*]	22.33 [*]

TTP, 6MOP, and 12MOP in the above table represent test tube plantlets, 6-month-old plants, and 12-month-old plants, respectively. Different letters within each column (parameter) indicate significant mean differences at $p \leq 0.05$, which are separated according to factors and their interaction. Data are the mean of ten independent biological replicates, whereas \pm data represent the standard deviation within replicates. The statistical analysis is based on a two-factorial completely randomized design. The multiple comparisons of means were performed by the least significance difference (LSD) test, where NS represents the non-significant difference and * shows a significant difference within the means at a 5% probability level.

4. Discussion

To produce identical pathogen-free plants for the agricultural industry, in vitro vegetative plant propagation is currently a cutting-edge biotechnology technique. Although the production of many economically important crops is still restricted by in vitro technology, much research has been undertaken to improve the unique in vitro culture media and micro-environment [24,25]. High concentrations of micro- and macronutrients, RH and sugar content, plant growth regulators, low light intensity, low osmotic and water potentials in the medium, and limited carbon dioxide and oxygen gas exchange are all factors that positively impact the in vitro growing plants [22,23]. These variables achieve high proliferation rates, but they also frequently result in physiological, anatomical, and morphological disorders that impede ex vitro acclimatization and decrease the survival rate of plants [72,73]. High proliferation rates during the in vitro multiplication stage, successful ex vitro acclimatization of the plantlets, high plant survival rates, and some degree of automation are all necessary for effective commercial in vitro propagation [74]. Successful acclimatization creates the ideal conditions for greater survival, subsequent growth, and the establishment of in vitro raised plantlets.

The influence of innovative technology in the agricultural sector is becoming more and more apparent every day. The inception of IoT-based automation has had a significant impact on the agricultural industry; it is not just restricted to the fields of crop production and diagnostics but has also impacted the modification of agricultural practices [75,76]. Internet of Things-based automation technology is applied to regulate plant tissue culture microclimate variables such as temperature, RH, and light [61–63]. However, very limited research work has been conducted into the use of this technology at the plantlet acclimatization stage where the mortality rate is considerably high.

The findings of the present study showed that plantlets transferred from in vitro conditions to E-VAS for acclimatization had a lower mortality rate than TGAS. After one month, the plantlets acclimatized in E-VAS had 67% lower mortality than the plantlets transferred to TGAS. Similarly, after six months a 66% lower mortality rate was observed in EVAS compared to TGAS. Similarly, the morpho-physiological characteristics of the plantlets also improved in E-VAS automated chambers. This indicates that if appropriate automated technology is not followed, plantlets may desiccate quickly and die due to the environmental changes when they are transferred from an in vitro culture room to an ex vitro greenhouse [39].

In the present study, in vitro plantlets were transferred to E-VAS, an automated IoT-based environment-controlled chamber. They were subjected to a congenial environment to get them established. Because of the favorable microclimate, the plantlets showed the highest survival rate and superior morpho-physiological traits. However, the environmental data recorded in the glasshouse (TGAS) indicated that the newly emerged plantlets struggled hard to survive because of the variation in the ambient environment variables, which also negatively affected their morpho-physiological attributes. These results indicate that the proposed automated IoT-based environmental chamber can improve the survival rate of date palm plantlets during ex vitro acclimatization and enhance plant growth and physiological parameters. A sophisticated microcomputer-controlled acclimatization unit is recommended for ex vitro plantlets' hardening to determine the RH, temperature, light intensity, CO₂ concentration, and air flow rate. The automated unit can change all the facets of the environment by increment over time [77–79]. The IoT-based system installed to monitor the photoperiod, light intensity, and quality remotely improved plant height, leaf area, leaf number, and chlorophyll content in *Brassica chinensis* [80]. To optimize plant photosynthetic activities, Yuan et al. [81] designed and implemented an open IoT-based plant growth chamber to implement real-time commands to control environmental factors. The root zone temperature of lettuce grown in an aeroponic system was automatically controlled using a smart IoT-designed system by recording the real-time environmental parameters, which showed an optimization of lettuce growth characteristics [82].

Since excessive heat or humidity can cause widespread plant damage, controlling and monitoring the environment in a glasshouse is essential [83,84]. However, due to their negative effects on plant growth and development, fluctuations in ambient temperature and RH are detrimental during acclimatization [85,86]. The limited accuracy of the available sensors makes it difficult for smart greenhouses to optimize these parameters [87]. In vitro plantlets of coconut were successfully acclimatized in a culture compartment inside a glasshouse with natural light (0–250 $\mu\text{mol m}^{-2} \text{s}^{-1}$) and RH (40–95%) but controlled temperature (26 ± 5 °C). These plantlets showed the highest photosynthesis rate, dry weight and number of leaves compared to the glasshouse plantlets subjected to the fluctuating natural temperature (25–38 °C). Following a six month ex vitro acclimatization period, plantlets grown under temperature-controlled glasshouse conditions maintained higher rates of field survival and growth in terms of fresh weight, dry weight, and leaf number [88].

5. Conclusions

An ex vitro acclimatization system (E-VAS) for in vitro plantlets is tested and discussed in the current research work. It describes the design and implementation of an automated IoT-based environmental chamber. In the presented E-VAS chamber, real-time monitoring and control systems were used to manage microclimate factors including temperature, RH, air quality, and light intensity. Additionally, using the appropriate sensors, the potting substrate's pH and moisture content were also monitored. Utilizing an automated IoT-based system, the microclimate data of the E-VAS were recorded and automatically uploaded to the ThinkSpeak platform for decision making. By analyzing the results of the implementation, it can be concluded that the designed system operated as expected. In comparison to TGAS, the in vitro-raised date palm (cv. Khalas) had a much higher survival rate. Moreover, E-VAS-acclimatized plants had much better morpho-physiological

characteristics. The proposed automated system has significant potential to meet the growing demand for the rapid multiplication of planting saplings produced through tissue culture because the plant growth-related parameters and survival rate were significantly higher in E-VAS than in the TGAS system that the industry currently uses for commercial production. To acclimatize mass-scale in vitro plantlets, the glasshouse can be equipped with the ex vitro acclimatization chamber or the IoT-based automated system can be used commercially in the glasshouse to reduce plantlet mortality. Plant scientists can manipulate the microclimate using the findings of this study to accommodate the requirements of various plant species. Additionally, the E-VAS chamber's CO₂ supply can be increased to enhance photosynthetic activities that can be monitored using CO₂ sensors, facilitating scientific studies on the regulation of photosynthesis.

Author Contributions: Conceptualization, M.M. (Maged Mohammed), M.M. (Muhammad Munir) and H.S.G.; methodology, M.M. (Maged Mohammed) and M.M. (Muhammad Munir); system design and manufacturing, M.M. (Maged Mohammed); software, M.M. (Maged Mohammed); validation, M.M. (Maged Mohammed) and M.M. (Muhammad Munir); formal analysis, M.M. (Maged Mohammed); investigation, M.M. (Maged Mohammed), M.M. (Muhammad Munir) and H.S.G.; data curation, M.M. (Maged Mohammed) and M.M. (Muhammad Munir); writing—original draft preparation, M.M. (Maged Mohammed) and M.M. (Muhammad Munir); writing—review and editing, M.M. (Maged Mohammed) and M.M. (Muhammad Munir); visualization, M.M. (Maged Mohammed); project administration, M.M. (Maged Mohammed); funding acquisition, M.M. (Maged Mohammed). All authors have read and agreed to the published version of the manuscript.

Funding: This work was supported by the Deanship of Scientific Research, Vice Presidency for Graduate Studies and Scientific Research, King Faisal University, Saudi Arabia (Grant No. GRANT1150).

Institutional Review Board Statement: Not applicable.

Informed Consent Statement: Not applicable.

Data Availability Statement: The data are available upon request from corresponding author.

Acknowledgments: The authors appreciate the logistic support and the availability of the engineering workshops for conducting this study, made possible by the Date Palm Research Center of Excellence, King Faisal University, Saudi Arabia.

Conflicts of Interest: All authors declare no conflict of interest.

References

1. Al-Khayri, J.M. Date Palm Phoenix Dactylifera L. In *Protocol for Somatic Embryogenesis in Woody Plants*; Jain, S.M., Gupta, P.K., Eds.; Springer: Dordrecht, The Netherlands, 2005; pp. 309–319. ISBN 978-1-4020-2985-1.
2. Zaid, A.; De Wet, P.F. Date Palm Cultivation. In *FAO Plant Production and Protection Paper 156 Rev.1*; FAO: Rome, Italy, 2002; pp. 1–28.
3. Chao, C.C.T.; Krueger, R.R. The date palm (Phoenix dactylifera L.): Overview of biology, uses, and cultivation. *HortScience* **2007**, *42*, 1077–1082. [[CrossRef](#)]
4. Torres, K.C. Application of Tissue Culture Techniques to Horticultural Crops. In *Tissue Culture Techniques for Horticultural Crops*; Springer: Boston, MA, USA, 1989; pp. 66–69.
5. Oseni, O.M.; Pande, V.; Nailwal, T.K. A Review on Plant Tissue Culture, A Technique for Propagation and Conservation of Endangered Plant Species. *Int. J. Curr. Microbiol. Appl. Sci.* **2018**, *7*, 3778–3786. [[CrossRef](#)]
6. Krishnaraj, S.; Vasil, I.K. Somatic Embryogenesis in Herbaceous Monocots. In *In Vitro Embryogenesis in Plants*; Thorpe, T.A., Ed.; Springer: Dordrecht, The Netherlands, 1995; pp. 417–470. ISBN 978-94-011-0485-2.
7. Wang, J.; Seliskar, D.M.; Gallagher, J.L. Plant regeneration via somatic embryogenesis in the brackish wetland monocot *Scirpus robustus*. *Aquat. Bot.* **2004**, *79*, 163–174. [[CrossRef](#)]
8. Carter, J.; Gunawardena, A.H. Regeneration of the aquatic monocot *Aponogeton madagascariensis* (lace plant) through callus induction. *Aquat. Bot.* **2011**, *94*, 143–149. [[CrossRef](#)]
9. Rajmohan, K. Date Palm Tissue Culture: A Pathway to Rural Development. In *Date Palm Biotechnology*; Jain, S.M., Al-Khayri, J.M., Johnson, D.V., Eds.; Springer: Dordrecht, The Netherlands, 2011; pp. 29–45. ISBN 978-94-007-1318-5.
10. Mohan Jain, S. Date palm biotechnology: Current status and prospective—an overview. *Emir. J. Food Agric.* **2012**, *24*, 386–399.
11. Aleid, S.M.; Al-Khayri, J.M.; Al-Bahrany, A.M. *Date Palm Status and Perspective in Saudi Arabia*; Al-Khayri, J.M., Jain, S.M., Johnson, D.V., Eds.; Springer: Dordrecht, The Netherlands, 2015; ISBN 978-94-017-9706-1.
12. Intha, N.; Chairprasart, P. Micropropagation of “KL1” date palm (Phoenix dactylifera L.). *Agric. Nat. Resour.* **2020**, *54*, 79–84.

13. Zayed, E.M.M.; Abd Elbar, O.H. Morphogenesis of immature female inflorescences of date palm in vitro. *Ann. Agric. Sci.* **2015**, *60*, 113–120. [[CrossRef](#)]
14. Shareef, H.J.; Muhsen, K.A.; Alhamd, A.D. Improving the germination of somatic embryos in date palm Berhi cultivar in vitro. *Int. J. Agron. Agric. Res.* **2016**, *8*, 17–23.
15. Al-Khayri, J.M.; Naik, P.M. Date palm micropropagation: Advances and applications. *Ciência E Agrotecnologia* **2017**, *41*, 347–358. [[CrossRef](#)]
16. Hassan, M.M.; Allam, M.A.; Shams El Din, I.M.; Malhat, M.H.; Taha, R.A. High-frequency direct somatic embryogenesis and plantlet regeneration from date palm immature inflorescences using picloram. *J. Genet. Eng. Biotechnol.* **2021**, *19*, 1–11. [[CrossRef](#)]
17. Abahmane, L. Date Palm Micropropagation via Organogenesis. In *Date Palm Biotechnology*; Jain, S.M., Al-Khayri, J.M., Johnson, D.V., Eds.; Springer: Dordrecht, The Netherlands, 2011; pp. 69–90.
18. Fki, L.; Kriaa, W.; Nasri, A.; Baklouti, E.; Chkir, O.; Masmoudi, R.B.; Rival, A.; Drira, N. Indirect Somatic Embryogenesis of Date Palm Using Juvenile Leaf Explants and Low 2,4-D Concentration. In *Methods in Molecular Biology*; Al-Khayri, J.M., Jain, S.M., Johnson, D.V., Eds.; Humana Press: New York, NY, USA, 2017; Volume 1637, pp. 99–106.
19. Al-Khayri, J.M. Somatic Embryogenesis of Date Palm (*Phoenix dactylifera* L.) from Shoot Tip Explants. In *Step Wise Protocols for Somatic Embryogenesis of Important Woody Plants: Volume II*; Jain, S.M., Gupta, P., Eds.; Springer International Publishing: Cham, Switzerland, 2018; pp. 231–244. ISBN 978-3-319-79087-9.
20. Sutter, E.G.; Shackel, K.; Diaz, J.C. Acclimatization of Tissue Cultured Plants. *Acta Hort.* **1992**, *23*, 115–120. [[CrossRef](#)]
21. Phillips, G.C.; Garda, M. Plant tissue culture media and practices: An overview. *Vitr. Cell. Dev. Biol. Plant.* **2019**, *55*, 242–257. [[CrossRef](#)]
22. Chandra, S.; Bandopadhyay, R.; Kumar, V.; Chandra, R. Acclimatization of tissue cultured plantlets: From laboratory to land. *Biotechnol. Lett.* **2010**, *32*, 1199–1205. [[CrossRef](#)]
23. Mahendra, R.; Chauhan, N.; Sharma, J.B.; Rana, K.; Bakshi, M. Ex-vitro Establishment of Tissue Cultured plants in Fruit Crops-A Review. *Int. J. Curr. Microbiol. Appl. Sci.* **2020**, *9*, 3321–3329. [[CrossRef](#)]
24. Benson, E.E. Special symposium: In vitro plant recalcitrance in vitro plant recalcitrance: An introduction. *Vitr. Cell. Dev. Biol. Plant.* **2000**, *36*, 141–148. [[CrossRef](#)]
25. Bidabadi, S.S.; Jain, S.M. Cellular, Molecular, and Physiological Aspects of In Vitro Plant Regeneration. *Plants* **2020**, *9*, 702. [[CrossRef](#)]
26. Hazarika, B.N. Acclimatization of tissue-cultured plants. *Curr. Sci.* **2003**, *85*, 1704–1712. [[CrossRef](#)]
27. Conover, C.A.; Poole, R.T. Acclimatization of Indoor Foliage Plants. In *Horticultural Reviews*; Janick, J., Ed.; John Wiley & Sons, Inc.: Hoboken, NJ, USA, 1984; pp. 119–154. ISBN 9781118060797.
28. Fuentes, G.; Talavera, C.; Espadas, F.; Quiroz, A.; Aguilar, M.; Coello, J.; Santamaría, J.M. Manipulation of abiotic in vitro factors to improve the physiology and subsequent field performance of micropropagated plantlets. *Acta Hort.* **2007**, *748*, 77–85. [[CrossRef](#)]
29. Joshi, P.; Joshi, N.; Purohit, S.D. Stomatal characteristics during micropropagation of *Wrightia tomentosa*. *Biol. Plant.* **2006**, *50*, 275–278. [[CrossRef](#)]
30. Đurković, J.; Lengyelová, A.; Čaňová, I.; Kurjak, D.; Hladká, D. Photosynthetic performance and stomatal characteristics during ex vitro acclimatization of true service tree (*Sorbus domestica* L.). *J. Hort. Sci. Biotechnol.* **2009**, *84*, 223–227. [[CrossRef](#)]
31. Sáez, P.L.; Bravo, L.A.; Sánchez-Olate, M.; Bravo, P.B.; Ríos, D.G. Effect of Photon Flux Density and Exogenous Sucrose on the Photosynthetic Performance during *In Vitro* Culture of *Castanea sativa*. *Am. J. Plant. Sci.* **2016**, *7*, 2087–2105. [[CrossRef](#)]
32. Cardoso, J.C.; Rossi, M.L.; Rosalem, I.B.; Teixeira da Silva, J.A. Pre-acclimatization in the greenhouse: An alternative to optimizing the micropropagation of gerbera. *Sci. Hort.* **2013**, *164*, 616–624. [[CrossRef](#)]
33. Kadleček, P.; Tichá, I.; Haisel, D.; Apková, V.; Schäfer, C. Importance of in vitro pretreatment for ex vitro acclimatization and growth. *Plant. Sci.* **2001**, *161*, 695–701. [[CrossRef](#)]
34. Hronková, M.; Zahradníčková, H.; ŠIMKOVÁ, M.; Šimek, P.; Heydová, A. The role of abscisic acid in acclimation of plants cultivated in vitro to ex vitro conditions. *Biol. Plant.* **2003**, *46*, 535–541. [[CrossRef](#)]
35. Pospíšilová, J.; Tichá, I.; Kadleček, P.; Haisel, D.; Plzánková, Š. Acclimatization of micropropagated plants to ex vitro conditions. *Biol. Plant.* **1999**, *42*, 481–497. [[CrossRef](#)]
36. Clapa, D.; Fira, A.; Joshee, N. An efficient ex vitro rooting and acclimatization method for horticultural plants using float hydroculture. *HortScience* **2013**, *48*, 1159–1167. [[CrossRef](#)]
37. Monja-Mio, K.M.; Olvera-Casanova, D.; Herrera-Herrera, G.; Herrera-Alamillo, M.Á.; Sánchez-Teyer, F.L.; Robert, M.L. Improving of rooting and ex vitro acclimatization phase of *Agave tequilana* by temporary immersion system (BioMINT™). *Vitr. Cell. Dev. Biol. Plant.* **2020**, *56*, 662–669. [[CrossRef](#)]
38. Premkumar, A.; Mercado, J.A.; Quesada, M.A. Effects of in vitro tissue culture conditions and acclimatization on the contents of Rubisco, leaf soluble proteins, photosynthetic pigments, and C/N ratio. *J. Plant. Physiol.* **2001**, *158*, 835–840. [[CrossRef](#)]
39. Kshitij Kumar, I.U.R. Morphophysiological Problems in Acclimatization of Micropropagated Plants in—*Ex Vitro* Conditions- A Reviews. *J. Orn. Hort. Plants* **2016**, *4*, 1–23.
40. Solangi, N.; Jatoi, M.A.; Markhand, G.S.; Abul-Soad, A.A.; Solangi, M.A.; Jatt, T.; Mirbahar, A.A.; Mirani, A.A. Optimizing Tissue Culture Protocol for In Vitro Shoot and Root Development and Acclimatization of Date Palm (*Phoenix dactylifera* L.) Plantlets. *Erwerbs Obstbau* **2022**, *64*, 97–106. [[CrossRef](#)]

41. Abul-Soad, A.A.; Jatoi, M.A. Factors affecting in vitro rooting of date palm (*Phoenix dactylifera* L.). *Pak. J. Agric. Sci.* **2014**, *51*, 477–484.
42. Pushpakanth, P.; Krishnamoorthy, R.; Anandham, R.; Senthilkumar, M. Biotization of tissue culture banana plantlets with *Methylobacterium salsuginis* to enhance the survival and growth under greenhouse and open environment condition. *J. Environ. Biol.* **2021**, *42*, 1452–1460. [[CrossRef](#)]
43. Wardle, K.; Dobbs, E.B.; Short, K.C. In Vitro Acclimatization of Aseptically Cultured Plantlets to Humidity. *J. Am. Soc. Hortic. Sci.* **2022**, *108*, 386–389. [[CrossRef](#)]
44. Hazarika, B.N.; da Silva, J.A.T.; Talukdar, A. Effective Acclimatization of in Vitro Cultured Plants: Methods, Physiology and Genetics. In *Floriculture, Ornamental and Plant Biotechnology*; da Silva, J.A.T., Ed.; Global Science Books: Bexhill-on-Sea, UK, 2006; Volume 2, pp. 427–438.
45. Mozas-Moral, A.; Bernal-Jurado, E.; Fernández-Uclés, D.; Medina-Viruel, M. Innovation as the Backbone of Sustainable Development Goals. *Sustainability* **2020**, *12*, 4747. [[CrossRef](#)]
46. Edan, Y.; Han, S.; Kondo, N. Automation in Agriculture. In *Springer Handbook of Automation*; Nof, S., Ed.; Springer: Berlin/Heidelberg, Germany, 2009; pp. 1095–1128.
47. Elhassan Ahmed, O.M.; Osman, A.A.; Awadalkarim, S.D. A Design of an Automated Fertigation System Using IoT. In Proceedings of the 2018 International Conference on Computer, Control, Electrical, and Electronics Engineering (ICCCEEE), IEEE, Khartoum, Sudan, 12–14 August 2018; pp. 1–5.
48. Mohammed, M.; Riad, K.; Alqahtani, N. Efficient iot-based control for a smart subsurface irrigation system to enhance irrigation management of date palm. *Sensors* **2021**, *21*, 3942. [[CrossRef](#)]
49. Lavanya, G.; Rani, C.; Ganeshkumar, P. An automated low cost IoT based Fertilizer Intimation System for smart agriculture. *Sustain. Comput. Inform. Syst.* **2020**, *28*, 100300. [[CrossRef](#)]
50. Rehman, A.; Saba, T.; Kashif, M.; Fati, S.M.; Bahaj, S.A.; Chaudhry, H. A Revisit of Internet of Things Technologies for Monitoring and Control Strategies in Smart Agriculture. *Agronomy* **2022**, *12*, 127. [[CrossRef](#)]
51. Chu, I. Economic analysis of automated micropropagation. In *Automation and Environmental Control in Plant Tissue Culture*; Springer: Dordrecht, The Netherlands, 1995; pp. 19–27.
52. Ilan, A.; Khayat, E. An overview of commercial and technological limitations to marketing of micropropagated plants. *Acta Hortic.* **1997**, *447*, 643–648. [[CrossRef](#)]
53. Leifert, C.; Cassells, A.C. Microbial hazards in plant tissue and cell cultures. *Vitr. Cell. Dev. Biol. Plant.* **2001**, *37*, 133–138. [[CrossRef](#)]
54. Huang, Y.J.; Lee, F.F. An automatic machine vision-guided grasping system for Phalaenopsis tissue culture plantlets. *Comput. Electron. Agric.* **2010**, *70*, 42–51. [[CrossRef](#)]
55. Zhao, J.C.; Zhang, J.F.; Feng, Y.; Guo, J.X. The study and application of the IOT technology in agriculture. In Proceedings of the 2010 3rd IEEE International Conference on Computer Science and Information Technology, ICCSIT, Chengdu, China, 9–11 July 2010; Volume 2, pp. 462–465.
56. Patil, V.C.; Al-Gaadi, K.A.; Biradar, D.P.; Rangaswamy, M. Internet of Things (Iot) and Cloud Computing for Agriculture: An Overview. *AgroInform. Precis. Agric.* **2012**, *1*, 292–296.
57. Muangprathub, J.; Boonnam, N.; Kajornkasirat, S.; Lekbangpong, N.; Wanichsombat, A.; Nillaor, P. IoT and agriculture data analysis for smart farm. *Comput. Electron. Agric.* **2019**, *156*, 467–474. [[CrossRef](#)]
58. Salam, A. Internet of Things for Sustainable Community Development: Introduction and Overview. In *Internet of Things*; Salam, A., Ed.; Springer International Publishing: Cham, Switzerland, 2020; pp. 1–31. ISBN 978-3-030-35291-2.
59. Memić, B.; Hasković Džubur, A.; Avdagić-Golub, E. Green IoT: Sustainability environment and technologies. *Sci. Eng. Technol.* **2022**, *2*, 24–29. [[CrossRef](#)]
60. Mohammed, M.; Riad, K.; Alqahtani, N. Design of a Smart IoT-Based Control System for Remotely Managing Cold Storage Facilities. *Sensors* **2022**, *22*, 4680. [[CrossRef](#)]
61. Dalina, D.U.; Sobejana, N. Automated Relative Humidity and Temperature Control System for Banana Tissue Culture Laboratory with Monitoring System and SMS Notification. *SSRN Electron. J.* **2019**, *5*, 6070. [[CrossRef](#)]
62. Memon, M.H. Design of Centralized Intelligent Expert System and Contamination Detection of Tissue Cultured Sugarcane Crop. *Sukkur IBA J. Emerg. Technol.* **2021**, *4*, 47–63. [[CrossRef](#)]
63. Widiawan, B.; Erawati, D.N.; Firgiyanto, R.; Anugro, A.P. Portable Device for Monitoring System in Network Culture Laboratory based on IoT. *Food Agric. Sci. Polije Proc. Ser.* **2021**, *3*, 119–127.
64. Mohammed, M.; Alqahtani, N.; El-Shafie, H. Development and Evaluation of an Ultrasonic Humidifier to Control Humidity in a Cold Storage Room for Postharvest Quality Management of Dates. *Foods* **2021**, *10*, 949. [[CrossRef](#)]
65. Mohammed, M.; El-Shafie, H.; Alqahtani, N. Design and Validation of Computerized Flight-Testing Systems with Controlled Atmosphere for Studying Flight Behavior of Red Palm Weevil, *Rhynchophorus ferrugineus* (Olivier). *Sensors* **2021**, *21*, 2112. [[CrossRef](#)]
66. Sagheer, A.; Mohammed, M.; Riad, K.; Alhajhoj, M. A cloud-based IoT platform for precision control of soilless greenhouse cultivation. *Sensors* **2021**, *21*, 223. [[CrossRef](#)]
67. Elshibli, S.; Elshibli, E.M.; Korpelainen, H. Growth and photosynthetic CO₂ responses of date palm plants to water availability. *Emir. J. Food Agric.* **2016**, *28*, 58–65. [[CrossRef](#)]

68. Abul-Soad, A.A. Micropropagation of Date Palm Using Inflorescence Explants. In *Date Palm Biotechnology*; Jain, S., Al-Khayri, J., Johnson, D., Eds.; Springer: Dordrecht, The Netherlands, 2011; pp. 91–117. [CrossRef]
69. Ahmed Mohammed, M.E.; Refdan Alhajhoj, M.; Ali-Dinar, H.M.; Munir, M. Impact of a Novel Water-Saving Subsurface Irrigation System on Water Productivity, Photosynthetic Characteristics, Yield, and Fruit Quality of Date Palm under Arid Conditions. *Agronomy* **2020**, *10*, 1265. [CrossRef]
70. Mohammed, M.; Munir, M.; Aljabr, A. Prediction of Date Fruit Quality Attributes during Cold Storage Based on Their Electrical Properties Using Artificial Neural Networks Models. *Foods* **2022**, *11*, 1666. [CrossRef] [PubMed]
71. ThingSpeak. LoT Analytics—ThingSpeak Internet of Things. Available online: <https://thingspeak.com/> (accessed on 17 September 2022).
72. Al-Mazroui, H.S.; Zaid, A.; Bouhouche, N. Morphological abnormalities in tissue culture-derived date palm (*Phoenix dactylifera* L.). In *Proceedings of the Acta Horticulturae*; III International Date Palm Conference, International Society for Horticultural Science: Abu Dhabi, United Arab Emirates, 2007; Volume 736, pp. 329–335.
73. Ruffoni, B.; Savona, M. Physiological and biochemical analysis of growth abnormalities associated with plant tissue culture. *Hortic. Environ. Biotechnol.* **2013**, *54*, 191–205. [CrossRef]
74. Lee, T.J.; Zobayed, S.; Firmani, F.; Park, E.J. A novel automated transplanting system for plant tissue culture. *Biosyst. Eng.* **2019**, *181*, 63–72. [CrossRef]
75. Mahant, M.; Shukla, A.; Dixit, S.; Patel, D. Uses of ICT in Agriculture. *Int. J. Adv. Comput. Res.* **2012**, *2*, 46–49.
76. Narinbaeva, G.; Menglikulov, B.; Siddikov, Z.; Bustonov, K.; Davlatov, S. Application of innovative technologies in agriculture of Uzbekistan. *E3S Web Conf.* **2021**, *284*, 02009. [CrossRef]
77. Maene, L.; Debergh, P. Liquid medium additions to established tissue cultures to improve elongation and rooting in vivo. *Plant. Cell. Tissue Organ. Cult.* **1985**, *5*, 23–33. [CrossRef]
78. Kozai, T.; Oki, H.; Fujiwara, K. Effect of CO₂ enrichment and sucrose concentration under high photosynthetic photon fluxes on growth of tissue cultured cymbidium plantlet during the preparation stage in plant micropropagation in horticulture industries. In *Plant Micropropagation in Horticultural Industries*; Ducate, G., Jacobs, M., Simpson, A., Eds.; Arlon, University Press: Liege, Belgium, 1987; pp. 135–141.
79. Kozai, T. High technology in protected cultivation from environmental control engineering point of view. In *Horticulture in High Technology*; Era, Special Lecture; Organizing Committee of International Symposium on High Technology in Protected Cultivation: Tokyo, Japan, 1988; pp. 1–43.
80. Harun, A.N.; Mohamed, N.; Ahmad, R.; Rahim, A.R.A.; Ani, N.N. Improved Internet of Things (IoT) monitoring system for growth optimization of Brassica chinensis. *Comput. Electron. Agric.* **2019**, *164*, 104836. [CrossRef]
81. Yuan, S.; Tang, H.; Fu, L.J.; Tan, J.L.; Govindjee, G.; Guo, Y. An open Internet of Things (IoT)-based framework for feedback control of photosynthetic activities. *Photosynthetica* **2022**, *60*, 79–87. [CrossRef]
82. Mohamed, T.M.K.; Gao, J.; Tunio, M. Development and experiment of the intelligent control system for rhizosphere temperature of aeroponic lettuce via the Internet of Things. *Int. J. Agric. Biol. Eng.* **2022**, *15*, 225–233. [CrossRef]
83. Rojas-Rishor, A.; Flores-Velazquez, J.; Villagran, E.; Aguilar-Rodríguez, C.E. Valuation of Climate Performance of a Low-Tech Greenhouse in Costa Rica. *Processes* **2022**, *10*, 693. [CrossRef]
84. Chauhan, K.K.; Lunagaría, M.M. Interpolation of Microclimatic Parameters Over Capsicum Under Open Ventilated Greenhouse. *Int. J. Econ. Plants* **2022**, *9*, 095–100. [CrossRef]
85. Muhl, Q.E.; Du Toit, E.S.; Robbertse, P.J. Moringa oleifera (Horseradish tree) leaf adaptation to temperature regimes. *Int. J. Agric. Biol.* **2011**, *13*, 1021–1024.
86. Zhu, L.; Bloomfield, K.J.; Asao, S.; Tjoelker, M.G.; Egerton, J.J.G.; Hayes, L.; Weerasinghe, L.K.; Creek, D.; Griffin, K.L.; Hurry, V.; et al. Acclimation of leaf respiration temperature responses across thermally contrasting biomes. *New Phytol.* **2021**, *229*, 1312–1325. [CrossRef] [PubMed]
87. Ryder, N.L.; Geiman, J.A.; Weckman, E.J. Hierarchical Temporal Memory Continuous Learning Algorithms for Fire State Determination. *Fire Technol.* **2021**, *57*, 2905–2928. [CrossRef]
88. Talavera, C.; Contreras, F.; Espadas, F.; Fuentes, G.; Santamaría, J.M. Cultivating in vitro coconut palms (*Cocos nucifera*) under glasshouse conditions with natural light, improves in vitro photosynthesis nursery survival and growth. *Plant. Cell. Tissue Organ. Cult.* **2005**, *83*, 287–292. [CrossRef]

Disclaimer/Publisher’s Note: The statements, opinions and data contained in all publications are solely those of the individual author(s) and contributor(s) and not of MDPI and/or the editor(s). MDPI and/or the editor(s) disclaim responsibility for any injury to people or property resulting from any ideas, methods, instructions or products referred to in the content.